

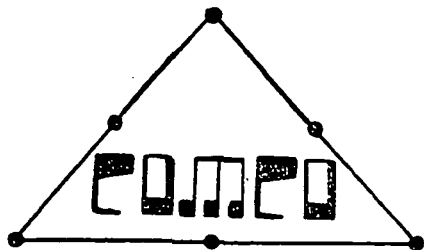
FINAL REPORT  
ON  
**ADAPTIVE COMPUTATIONAL  
METHODS FOR SSME  
INTERNAL FLOW ANALYSIS**

NASA CONTRACT NA8-36647

MARSHALL SPACE FLIGHT CENTER, NASA

BY J. TINSLEY ODEN

TR86-05



THE COMPUTATIONAL MECHANICS COMPANY, INC.

THE COMPUTATIONAL  
MECHANICS CO., INC.  
4804 AVENUE H  
AUSTIN, TEXAS 78751

(NASA-CR-178864) ADAPTIVE COMPUTATIONAL  
METHODS FOR SSME INTERNAL FLOW ANALYSIS  
Final Report (Computational Mechanics  
Consultants) 58 F

CSCL 20D

N86-30959

Unclas

G3/34 43374

## TABLE OF CONTENTS

FOREWORD .....	1
1. INTRODUCTION .....	2
2. SPACE-TIME VARIATIONAL FORMULATION OF COMPLEX FLOW PROBLEMS .....	5
2.1. A Space-Time Navier-Stokes Formulation .....	5
2.2. A Space-Time Variational Formulation of the Euler Equations .....	6
3. ADAPTIVE SCHEMES .....	10
3.1. Finite Element Approximations .....	10
3.2. A Node Redistribution Method .....	14
3.3. Numerical Experiments - An r-Method .....	20
3.4. A p-Method .....	32
4. CONCLUSIONS .....	39
REFERENCES .....	40
APPENDIX .....	41
REFERENCES FOR THIS APPENDIX .....	56

## FOREWORD

This document is the final report of work done on adaptive finite element methods for SSME internal flow analysis for NASA under Contract NAS8-36647. The results described here summarize a one-year pilot study into several classes of adaptive methods which may have important implications in a large body of computational fluid dynamics work connected with the analysis and design of the space shuttle main engine. The one-year effort supported by this NASA-Marshall Space Flight Center contract represents one component of a larger program on adaptive methods in CFD underway at the Computational Mechanics Company, Inc. of Austin, Texas. The very encouraging results obtained suggest that a significant increase in the reliability of computer-generated flow simulations is possible through the use of special error estimates and various adaptive procedures.

## 1. INTRODUCTION

In this report, we describe adaptive finite element methods for the analysis of classes of problems in compressible and incompressible flow of interest in SSME (space shuttle main engine) analysis and design.

The general objective of the adaptive methods of interest here is to improve and to quantify the quality of numerical solutions to the governing partial differential equations of fluid dynamics in two-dimensional cases. Implicit in this goal is the resolution of two questions: 1) how is this quality of the numerical solution to be assessed? and 2) how does one effectively adapt the solution to improve quality?

An answer to the first question is to somehow estimate the local error in a given mesh cell (in an appropriate norm) by using the results of a first trial calculation. Stated in another way, one can construct a-posteriori error estimates using data from rougher solutions obtained on a coarse mesh or with a low-order approximation. Once an estimate of the local quality of the solution is known, one can "adapt" the numerical scheme so as to improve the quality of the solution; i.e. so as to reduce the local approximation error.

There are several different families of adaptive schemes that can be used to improve the quality of solutions in complex flow simulations. Among these are 1) r-methods (node-redistribution or moving mesh methods) in which a fixed number of nodal points is allowed to migrate to points in the mesh where high error is detected; 2) h-methods, in which the mesh size  $h$  is automatically refined to reduce local error and 3) p-methods, in which the local degree  $p$  of the finite element approximation is increased

to reduce local error. There are, of course, combinations of these methods which can be very effective. Two of the three basic techniques have been studied in the project reported here: an r-method for steady Euler equations in two dimensions and a p-method for transient, laminar, viscous incompressible flow. For discussions of our work on h-methods for these types of problems see, e.g. [ 1, 2, 3, 4].

The issue of a-posteriori error estimation is a difficult one. Two basic categories of error estimation were studied in the work described here: 1) residual methods and 2) interpolation methods. The former classes of methods make use of residuals computed using trial finite element solutions. These methods can be computationally expensive; however, they can yield very good estimates of the local error. Interpolation methods, on the other hand, are easily implemented but may yield quite crude estimates of the actual error. These schemes employ interpolation theory and exploit superconvergence properties of finite element methods; they seem to be perfectly adequate as a basis for adaptive mesh schemes for the classes of problems considered here.

Following this Introduction, we present weak forms of Navier-Stokes equations and the Euler equations that are used as a basis for the development of finite element approximations. Since we anticipate the use of techniques which move nodes and elements, we construct general space-time "variational formulations" for these problems for which the computational domain can vary with time. In Section 3, we present two types of adaptive schemes. First, an r-method for two-dimensional steady problems in inviscid compressible flow characterized by the Euler equations. Numerical results are presented for some representative test problems. In Section 3, we

also outline a p-method for incompressible viscous flows and cite some preliminary numerical results. A brief introduction to residual methods of a-posteriori error estimation is given in an Appendix, and some pertinent conclusions of the study are listed in Section 4.

## 2. SPACE-TIME VARIATIONAL FORMULATIONS

### OF COMPLEX FLOW PROBLEMS

2.1. A Space-Time Navier-Stokes Formulation. A general space-time variational principle for incompressible viscous flow is characterized as follows (see [ 1, 2, 3]).

Find a velocity field  $u$  in a class of functions  $V$  such that over a time interval  $[ 0, T ]$ ,

$$\begin{aligned} & \int_0^T \{ \rho [ \mathbf{v}_t, \mathbf{u}^\varepsilon ]_t + \mu ( ( \mathbf{u}^\varepsilon, \mathbf{v} ) )_t + \rho b ( \mathbf{u}^\varepsilon, \mathbf{u}^\varepsilon, \mathbf{v} ) \\ & \quad + \varepsilon^{-1} ( \operatorname{div} \mathbf{u}^\varepsilon, \operatorname{div} \mathbf{v} )_t \} dt \\ & = \int_0^T ( \mathbf{f}, \mathbf{v} )_t dt + \rho ( \mathbf{u}, \mathbf{v} )_0 - \rho ( \mathbf{u}^\varepsilon, \mathbf{v} )_T \\ & \qquad \qquad \qquad \forall \mathbf{v} \in V \end{aligned} \tag{2.1}$$

where  $\mathbf{v}$  is an arbitrary test function,  $\rho$  the mass density,  $\mu$  the viscosity,  $\mathbf{f}$  the body force, and

$$\begin{aligned} [ \mathbf{v}_t, \mathbf{u} ]_t &= \int_{\Omega_t} \frac{\partial \mathbf{v}}{\partial t} \cdot \mathbf{u} \, dx \quad \text{at time } t \\ ( ( \mathbf{u}, \mathbf{v} ) )_t &= \int_{\Omega_t} \nabla \mathbf{u} : \nabla \mathbf{v} \, dx \quad \text{at time } t \\ ( \mathbf{u}, \mathbf{v} )_t &= \int_{\Omega_t} \mathbf{u} \cdot \mathbf{v} \, dx \quad \text{at time } t \\ b ( \mathbf{u}, \mathbf{u}, \mathbf{v} ) &= \bar{b} ( \mathbf{u}, \mathbf{u}, \mathbf{v} ) + \bar{b} ( \mathbf{u}, \psi, \mathbf{v} ) + \bar{b} ( \psi, \mathbf{u}, \mathbf{v} ) \\ \bar{b} ( \mathbf{u}, \mathbf{v}, \mathbf{w} ) &= \int_{\Omega_t} [ ( \mathbf{u} \cdot \nabla ) \mathbf{v} \cdot \mathbf{w} + \frac{1}{2} \operatorname{div} \mathbf{u} ( \mathbf{v} \cdot \mathbf{w} ) ] \, dx \end{aligned}$$

with  $\Omega_t$  the spatial time domain at time  $t$ . Here we use a penalty method (artificial compressibility) to approximate the hydrostatic pressure  $p$ , by

$$p_\epsilon = -\epsilon^{-1} \operatorname{div} \mathbf{u}_\epsilon$$

with  $\epsilon$  a small positive parameter. The functional  $b(\cdot, \cdot, \cdot)$  represents the convective term in the Navier-Stokes equations and  $\psi$  is a particular function designed to simplify the enforcement of no-flow boundary conditions.

A finite element approximation (2.1) is obtained by replacing  $\mathbf{u}^\epsilon$  and  $\mathbf{v}$  with appropriate discrete approximations defined over a space-time element  $K$ ; e.g.

$$\mathbf{u}^\epsilon \approx \mathbf{u}_h^\epsilon(\mathbf{x}, t) = \sum_N \mathbf{u}_\epsilon^N(t) \psi_N(\mathbf{x})$$

Once a finite element solution is obtained on a fixed mesh, we use it to compute a local error indicator  $\phi_K$  which bounds the local  $\mathbf{e}^h = \mathbf{u}^\epsilon - \mathbf{u}_h^\epsilon$  in an appropriate norm:

$$\|\mathbf{e}^h\|_K \leq \|\phi_K\| \quad \text{for element } K$$

We shall discuss means for obtaining  $\phi_K$  later.

## 2.2 A Space-Time Variational Formulation of the Euler Equations.

By following a plan similar to that used in the formulation of the weak-space-time problem (2.1), a space-time formulation of the Euler equations in two dimensions can be obtained.



If  $U(x,t)$ ,  $(x,t) \in D$ , is the 4-vector of conservation variables,  $U = \{\rho, m, E\}^T$ , with  $\rho$  the mass density,  $m$  the linear momentum, and  $E$  the total energy, and if  $d\Omega$  and  $dS$  denote Lebesgue measures of area (volume) and length (area) of  $\Omega$  and  $\partial\Omega$  respectively, then we demand that  $U$  satisfy the following system of conservation laws:

$$\frac{d}{dt} \int_{\Omega} U \, d\Omega = - \int_{\partial\Omega} Q(U) \underline{n} \, dS \quad (3.1)$$

Here,  $Q(U)$  is the flux and  $\underline{n}$  is the unit outward normal to  $\partial\Omega$ . If  $m_1, m_2$  denote Cartesian components of  $\underline{m}$ , then

$$\underline{U} = \{\rho, m_1, m_2, E\}^T$$

$$Q(U) = \left[ \begin{array}{c|c} m_1 & m_2 \\ \hline \rho^{-1} m_1^2 + p(U) & \rho^{-1} m_1 m_2 \\ \rho^{-1} m_1 m_2 & \rho^{-1} m_2^2 + p(U) \\ \hline \rho^{-1} m_1 (E + p(U)) & \rho^{-1} m_2 (E + p(U)) \end{array} \right]$$

$$\underline{n} = \{n_1, n_2\}^T; \quad p(U) = (\gamma - 1)(E - \rho^{-1} \underline{m} \cdot \underline{m}/2)$$

In these equations,  $p$  is the thermodynamic pressure and  $\gamma$  is the ratio of specific heats, assumed here to be constant. In addition to (3.1),  $U$  must satisfy an entropy production inequality as well as an initial condition,

$$\underline{U}(\underline{x}, 0) = \underline{U}_0(\underline{x}), \quad \underline{x} \in \Omega$$

where  $\underline{U}_0$  is given.

It is of fundamental importance to note the smoothness requirements on  $\underline{U}$  in order that (3.1) make sense mathematically. Conservation laws (3.1) hold when the components of  $\underline{U}$  are bounded measurable (with respect to Lebesgue measure in  $\underline{x}$ ) functions on  $D$ . Thus, we may seek solutions in the function space

$$V = \{ \underline{v} = \{v_1, v_2, v_3, v_4\}^T \mid v_i = v_i(\underline{x}, t) \\ \in L^\infty(0, T; L^1(\Omega)) ; i = 1, 2, 3, 4 \}$$

In particular, (3.1) is not equivalent to the classical Euler equations,  $\underline{U}_t + \text{div } \underline{Q}(\underline{U}) = \underline{0}$  (with  $\underline{U}_t = \partial \underline{U} / \partial t$  and  $\text{div } \underline{Q} = \sum_1 \partial Q_{\alpha i} / \partial x_i$ ) since solutions may not possess derivatives across surfaces in  $D$ . However, the conservation laws and initial conditions are fully equivalent to the following weak boundary-initial value problem:

Find  $\underline{U} \in V$  such that

$$\int_D (\underline{U}^T \phi_t + \underline{Q}(\underline{U}) : \underline{\nabla} \phi) d\Omega dt \\ + \int_\Omega \underline{U}_0^T \phi(\cdot, 0) d\Omega = \int_0^T \int_{\partial\Omega} \underline{F}^T \phi dS dt$$

for all  $\phi \in W$

where  $\underline{F}$  is the actual prescribed flux through  $\partial\Omega$  and  $W$  is a suitable space of test functions.

Here, we use the notation

$$\underline{U}^T \phi_t = \sum_{\alpha=1}^4 U_{\alpha} \frac{\partial \phi_{\alpha}}{\partial t} \quad ; \quad Q : \nabla \phi = \sum_{i=1}^2 \sum_{\alpha=1}^4 Q_{\alpha i} \frac{\partial \phi_{\alpha}}{\partial x_i}$$

Consider an arbitrary time interval  $[\tau_1, \tau_2] \subset [0, T]$  and include in  $W$  functions  $\phi(\underline{x}, \tau_2) \neq 0$ . Let  $\omega$  be a subset of  $\Omega$  such that  $\omega \cap \bigcup_k \Gamma_k = \emptyset$ , and let  $\underline{F} \equiv \underline{Qn}$ . Then another weak statement of the system conservation laws over  $\bar{\omega} \times [\tau_1, \tau_2]$  is:

Find  $\underline{U} \in V^{\omega, \tau}$  such that

$$\begin{aligned} & \int_{\tau_1}^{\tau_2} \int_{\omega} \left( -\underline{U}^T \phi_t + (\operatorname{div} \underline{Q})^T \phi \right) d\Omega \, dt \\ & + \int_{\omega} \left( \underline{U}^T(\cdot, \tau_2) \phi(\cdot, \tau_2) - \underline{U}^T(\cdot, \tau_1) \phi(\cdot, \tau_1) \right) d\Omega = 0 \end{aligned} \quad (2.2)$$

for all  $\phi \in W^{\omega, \tau}$

with  $V^{\omega, \tau}$  and  $W^{\omega, \tau}$  appropriate spaces of trial and test functions.

### 3. ADAPTIVE SCHEMES

3.1 Finite Element Approximations. A hierarchal finite element method designed for use in a p-method is used to construct approximations of (2.1). We furnish some details late in this section. For a more complete discussion of our approach, see [5].

Turning to (2.2), finite element approximations of the gas dynamics problem are obtained by a direct approximation on finite-dimensional spaces approximating the spaces  $V$  and  $W$ . The spatial domain  $\Omega$  is partitioned into a collection  $T_h$  of finite elements  $\Omega_e$  over which the components of trial functions  $\underline{v}$  are approximated by polynomials of degree  $k$ . In this way, we construct a family  $\{V_h\}$  of finite dimensional spaces of the type

$$V_h = \{ \underline{v}^h = \{v_1^h, v_2^h, v_3^h, v_4^h\}^T \in V \mid v_i^h \in P_k(\Omega_e), \quad i = 1, 2, 3, 4 \}$$

where  $P_k(\Omega_e)$  is the space of polynomials of degree  $k$  defined over  $\Omega_e$ . Alternatively, we can use  $v_i^h|_{\Omega_e} \in Q_k(\Omega_e)$ , where  $Q_k(\Omega_e)$  is the space of tensor products of polynomials of degree  $k$  on  $\Omega_e$  (e.g.,  $Q_1(\Omega_e)$  is spanned by bilinear functions,  $Q_2(\Omega_e)$  by biquadratics, etc.). In addition, a family  $\{W_h\}$  of finite dimensional spaces of test functions is also constructed. We then consider Galerkin approximations by seeking solutions in  $V_h$ , with  $W$  replaced by  $W_h$ .

We next derive a special semi-discrete, weak formulation which provides the basis for the construction of a popular family of finite element schemes. We proceed with the following steps:

- i) Partition the time interval  $[0, T]$  according to  $0 = t_0 < t_1 < t_2 < \dots < t_N = T$  ;
- ii) Apply the weak balance law (2.2) to a typical time interval  $[t_n, t_{n+1}]$  (with  $\tau_1 = t_n$  and  $\tau_2 = t_{n+1}$  ) ;
- iii) Set  $\phi_t = 0$  in (2.2) suggesting the ultimate use of a time-invariant grid (we relax this assumption later);
- iv) Replace the time integrations in (2.2) by the elementary midpoint quadrature rule

$$\int_{t_n}^{t_{n+1}} f(t) dt \approx \Delta t f^{n+\frac{1}{2}}$$

$$\Delta t = t_{n+1} - t_n, \quad f^{n+\frac{1}{2}} = f(t_n + \Delta t/2)$$

Thus, with  $\omega = \Omega$  , we obtain the semidiscrete approximation

$$\begin{aligned} \int_{\Omega} \phi_h^T \tilde{U}^{n+1} d\Omega &= \int_{\Omega} \phi_h^T \tilde{U}^n d\Omega + \Delta t \int_{\Omega} Q^{n+\frac{1}{2}} : \nabla \phi_h d\Omega \\ &\quad - \Delta t \oint_{\partial\Omega} \phi_h^T (Q^{n+\frac{1}{2}} \underline{n}) dS \end{aligned}$$

$$\text{for all } \phi_h \quad (3.1)$$

where  $\tilde{U}_h^n = U_h(\underline{x}, t_n)$  , etc.,  $\tilde{U}_h$  being the approximation of  $\underline{U}$  , and  $Q^{n+\frac{1}{2}}$  is the flux at the half step,

$$Q^{n+\frac{1}{2}} = Q(\tilde{U}_h^{n+\frac{1}{2}})$$

- v) To obtain an approximation  $\tilde{U}_h^{n+\frac{1}{2}}$  , we use (2.1) again for time interval  $[t_n, t_{n+\frac{1}{2}}]$  , this time replacing the time integrals by a simple strip rule and integrating by parts the divergence terms

$$\begin{aligned}
\int_{\Omega_e} \phi_h^T \tilde{U}_h^{n+1/2} d\Omega &= \int_{\Omega_e} \phi_h^T U_h^n d\Omega \\
&\quad - \frac{\Delta t}{2} \int_{\Omega_e} \phi_h^T (\text{div } Q^n) d\Omega
\end{aligned}$$

for all  $\phi_h$  (3.2)

We thus arrive at the algorithm,

- 1) With  $(U_h^n, Q^n = Q(U_h^n))$  known at the  $n$ th time step,  
compute  $\tilde{U}_h^{n+1/2}$  using (3.4)
- 2) Compute  $Q^{n+1/2}$  using (3.3)
- 3) Compute  $\tilde{U}_h^{n+1/2}$  using (3.4)
- 4) Go to 1)

This algorithm is the finite-element based two-step Lax-Wendroff/Taylor Galerkin scheme. It is one of a family of methods advanced by Donea [6], studied by Baker and Kim [7], and successfully refined and used by Löhner et al. [8,9] in finite-element applications in fluid dynamics. This semi-explicit method is of second order in time and can experience spurious oscillations near shocks and other types of irregularities in the solution. These deficiencies must be reckoned with in implementing the method, and for this purpose we append to the right-hand side of (3.1) an artificial term of the form

$$\begin{aligned}
& - \Delta t \int_{\Omega} \sum_{\alpha=1}^4 \sum_{i=1}^2 c_i(u) U_{\alpha,i}^{n+1} \phi_{\alpha,i}^h d\Omega \\
& - \Delta t \oint_{\partial\Omega} \phi_h^T (c(u^n) \cdot \nabla U^n) \cdot n \, ds
\end{aligned}$$

with

$$c_i(u) = C \frac{\partial u_i}{\partial x_i} \quad (\text{no sum on } i)$$

In this work, we use meshes of four-node quadrilaterals over which the components of  $U$  are piecewise bilinear functions. Similar approximations and algorithms are used by Bey et al. In addition, so-called group approximations of the flux  $Q_{\alpha i}$  ( $\alpha = 1, 2, 3, 4$ ;  $i = 1, 2$ ) are employed so that these components are also piecewise bilinear functions determined by their values at element nodes. In general, this finite element approximation will be of the form,

$$U_{\alpha} \approx \sum_{j=1}^N U_{\alpha}^j(t) \phi_j(\underline{x})$$

$$Q_{\alpha i} \approx \sum_{j=1}^N Q_{\alpha i}^j(t) \phi_j(\underline{x})$$

where  $N$  denotes the total number of nodes in the discretization, and  $U_{\alpha}^j$ ,  $Q_{\alpha i}^j$  are values of  $U^h$ ,  $Q^h$  at node  $j$ , and  $\phi_j$  are the global piecewise bilinear basis functions.

As noted earlier, we advance the solution in time in two steps. It is important to note that the first step is essentially local, computed over each element, while the second is global and contains the artificial viscosity terms:

First Step: For each element  $\Omega_e$ , calculate a constant element vector

$U_{\alpha, e}^{n+1/2}$  from

$$U_{\alpha, e}^{n+1/2} \int_{\Omega_e} d\Omega = \sum_{i=1}^4 \left\{ \left( \int_{\Omega_e} \phi_i d\Omega \right) U_{\alpha}^{i, n} - \frac{\Delta t}{2} \left( \int_{\Omega_e} \frac{\partial \phi_i}{\partial x_{\beta}} d\Omega \right) Q_{\alpha \beta}^{i, n} \right\}$$

Second Step: For each node  $j$ , calculate  $U_\alpha^{j,n+1}$  by solving the following system of equations

$$\begin{aligned} \sum_{j=1}^N \left\{ \int_{\Omega} \left( \phi_i \phi_j + \tau_\beta \frac{\partial \phi_i}{\partial x_\beta} \frac{\partial \phi_j}{\partial x_\beta} \right) d\Omega \right\} U_\alpha^{j,n+1} &= \sum_{j=1}^N \left( \int_{\Omega} \phi_i \phi_j d\Omega \right) U_\alpha^{j,n} \\ &+ \Delta t \int_{\Omega} Q_{\alpha\beta}^{n+1/2} \frac{\partial \phi_i}{\partial x_\beta} d\Omega - \Delta t \int_{\partial\Omega} n_\beta (Q_{\alpha\beta}^{n+1/2} - \bar{Q}_{\alpha\beta}^n) \phi_i ds \\ &- \Delta t \int_{\partial\Omega} n_\beta Q_{\alpha\beta}^n \phi_i ds \end{aligned}$$

Here,  $\bar{Q}^n$  denotes the elementwise averaged value of the flux. The coefficients  $\tau_\beta$  are defined to be constant over each element,

$$\tau_\beta = c A_e \left| \frac{\partial u_\beta^h}{\partial x_\beta} \right|$$

where  $c$  is a global constant ( $c = 1$  in the examples),  $A_e$  denotes the area of  $\Omega_e$ ,  $u_\beta^h$  denote the components of the fluid velocity.

3.2 A Node Redistribution Method. We now describe one of the principal aspects of this investigation: a moving-mesh, node-redistribution method based on equidistribution of error indicators. We begin by presenting a simpler mathematical justification of the concept of equidistribution of error.

Consider a regular mesh of quadrilateral elements  $\Omega_e$  with a diameter  $h_e$ . Let  $\theta_e$  be an error indicator for element  $e$  and suppose that the mesh contains a fixed number  $M$  of elements. Let  $h = h(x_1, x_2)$  be a mesh



function such that

$$h(x_1, x_2) = h_e = \text{dia}(\Omega_e) \quad \text{for } (x_1, x_2) \in \Omega_e$$

and note that, approximately,

$$M = \int_{\Omega} \frac{d\Omega}{h^2}$$

with  $d\Omega = dx_1 dx_2$  (this being exact for domains which are unions of square elements). Let  $\theta = \theta(x_1, x_2)$  be mesh function which gives the local error indicator when evaluated at a point ( $\theta = \theta_e$  for  $\underline{x} \in \Omega_e$ ). We wish to minimize the total error indicator functional,

$$J(\theta) = \sum_{e=1}^M \int_{\Omega} \theta_e^2 d\Omega$$

subject to the constraint (3.3). Using Lagrange multipliers, this leads to the optimality condition,

$$\delta \left( J + \lambda \left( \int_{\Omega} h^{-2} d\Omega - M \right) \right) = 0,$$

or

$$\sum_e 2 \int_{\Omega_e} \left( \theta_e \frac{\partial \theta}{\partial h} - \lambda h^{-3} \right) \delta h d\Omega = 0$$

or

$$h_e^3 \theta_e \frac{\partial \theta_e}{\partial h} - \lambda = 0$$

Suppose that  $\text{meas}(\Omega_e) = \sigma_0 h_e^2$  and that  $\theta_e$  is of the form  $\theta_e = h_e^\sigma f(u)$ . Then, integrating this last result over a typical element gives

$$\int_{\Omega_e} \sigma h_e^3 \theta_e h_e^{\sigma-1} f(u) d\Omega = \lambda \sigma_0 h_e^2$$

Hence, the optimal mesh size distribution results when

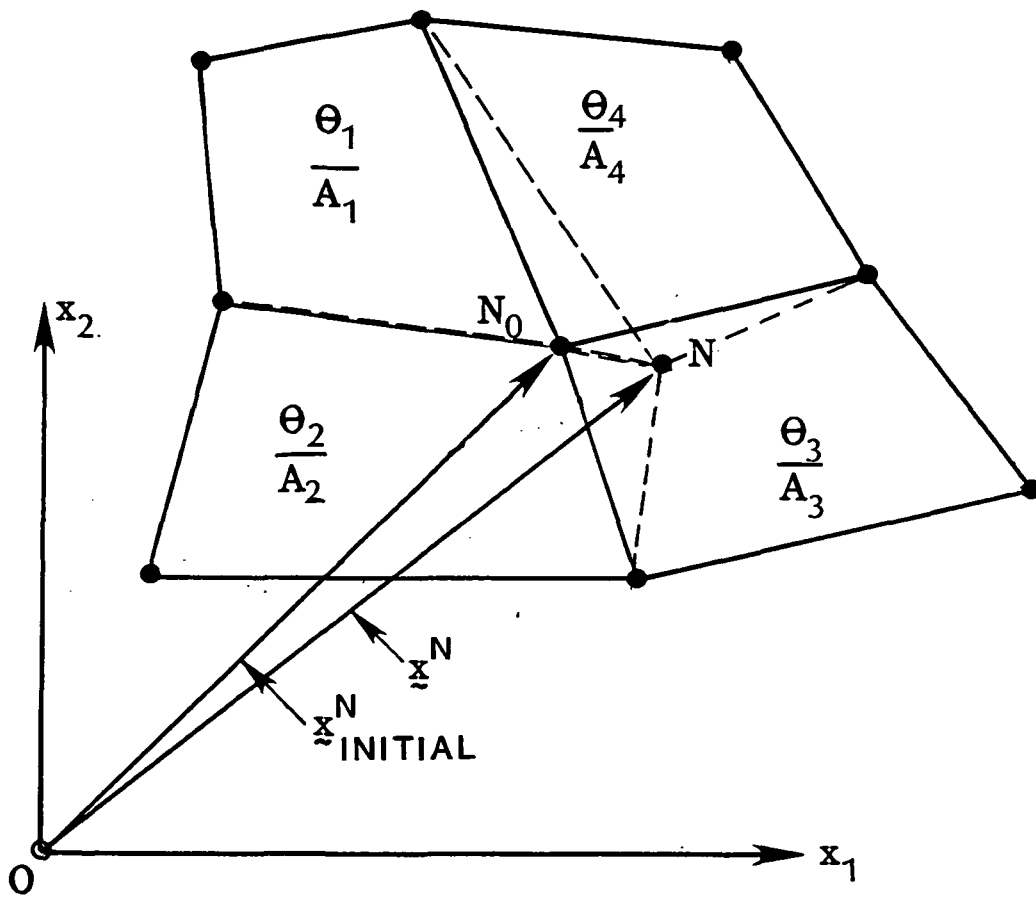


Figure 1. Calculation of area center-of-error  $\tilde{x}^N$  to equidistribute element error indicators in a cluster of four elements.

$$\int_{\Omega_e} \theta_e^2 d\Omega = \lambda \sigma_0 / \sigma = \text{CONST.} \quad (3.4)$$

In other words, to obtain the optimal mesh, we must equidistribute the indicators  $\int \theta_e^2$ .

To use this result to redistribute nodes, we proceed as follows (cf. Diaz et al. :

- 1) Generate an initial (generally regular) mesh with a fixed number  $M$  of elements and compute a trial solution on this mesh at one time step;
- 2) Compute the corresponding error indicators  $\theta_e$ ;
- 3) For a group  $k$  of  $P$  elements (with  $P$  always 4 in this work), let  $A_{e_i}$  denote the area of element  $i$  in the group. The area-weighted indicators for group  $k$  are the  $P$ -numbers,

$$\theta_{ei} / A_{ei}$$

- 4) Let  $\gamma_{e_i}$  denote a vector from the origin of a global coordinate system to the centroid of element  $e_i$  of group  $k$ . Then the center of error of group  $k$  is defined as the vector (see Fig. 1)

$$\tilde{x}^k = \frac{\sum_{i=1}^4 \gamma_{e_i} \left( \frac{\theta_{e_i}}{A_{e_i}} \right)}{\sum_{i=1}^4 \left( \frac{\theta_{e_i}}{A_{e_i}} \right)}$$

- 5) Relocate the node at the center of group  $k$  to lie at the vertex of  $\tilde{x}^k$ ;
- 6) Continue this sequence of operations over each group  $h$  of four elements until the new location of each node does not change more than a preassigned tolerance.

There remains only the issue of how the error indicator  $\theta_e$  can be calculated in an efficient manner. Instead of using residual methods such as those discussed in the Appendix, we shall use an interpolation method. These methods are derived from the theory of interpolation of finite elements (see Oden and Carey [10]). In particular, let  $u$  be a smooth function defined over a regular domain  $\Omega$ . The  $W^{r,p}(\Omega)$ -semi-norm of  $u$  is defined by

$$|u|_{W^{r,p}(\Omega)} = \left\{ \int_{\Omega} \sum_{\substack{i+j=r \\ i,j \geq 0}} \left| \frac{\partial^{i+j} u}{\partial x_1^i \partial x_2^j} \right|^p d\Omega \right\}^{1/p}$$

where  $1 \leq p \leq \infty$  and  $r$  is a non-negative integer.

The Sobolev norm of  $u$  is

$$\|u\|_{W^{r,p}(\Omega)_u} = \left\{ \sum_{k=0}^r |u|_{W^{k,p}(\Omega)}^p \right\}^{1/p}$$

Let  $G$  be an arbitrary convex subdomain (a finite element) of  $\Omega$  over which  $u$  is interpolated by a function  $\tilde{u}_h$  which contains complete piecewise polynomials of degree  $k$ . Then, it can be shown that the local interpolation error in the  $W^{m,p}(G)$ -semi-norm is

$$\begin{aligned} |u - \tilde{u}_h|_{W^{m,p}(G)} \\ \leq C \frac{h^{k+1}}{\rho^m} \cdot h^{\frac{n}{p} - \frac{n}{p}} |u|_{W^{k+1,p}(G)} \end{aligned}$$

where

$h$  = the diameter of the domain  $G$

$\rho$  = the diameter of the largest sphere that can be inscribed inside  $G$

$n$  = the dimension of the domain  $\Omega$

$$p' = p/(p - 1)$$

$C$  = a constant independent of  $h$ ,  $\rho$ , and  $u$ .

If  $\rho$  is proportional to  $h$  and if it remains proportional in refinements of  $G$  defined by parametrically reducing  $h$ , we have

$$|E^h|_{m,p,G} \leq C h^{\frac{n}{p'} - \frac{n}{p} + k+1 - m} |u|_{k+1,p} \quad (4.13)$$

with  $|\cdot|_{m,p,G} = |\cdot|_{W^{m,p}(G)}$ , etc. and  $E^h = u - \tilde{u}_h$ .

Such estimates can be used to devise crude adaptive schemes. Suppose that  $u$  on the right side of (4.13) is replaced by a finite element approximation  $u_h$  and that  $|u_h|_{k+1,p} = |u|_{k+1,p} + O(h)$ . Then, (3.4) indicates that the local error in the  $W^{m,p}(G)$  seminorm is proportional to the error indicator,  $h^{\frac{n}{p'} - \frac{n}{p} + k+1 - m} |u|_{k+1,p}$ . Some choices are:

$$i) \quad n = 2, \quad m = 0, \quad k = 1, \quad p = p' = 2$$

$$\|E^h\|_{L^2(G)} \leq C h^2 |u|_{2,2,G} = C \theta_G \quad (3.5)$$

In this case, one must approximate the  $W^{2,2}$ -semi-norm of  $u$  over  $G$ ; i.e., the  $L^2$ -norm of second partial derivatives of  $u$ .

$$ii) \quad n = 2, \quad p = \infty, \quad p' = 1, \quad k = 0, \quad m = 0.$$

$$\begin{aligned} |E^h|_{L^1(G)} &= Ch^2 |E^h_{\text{average}}| \\ &\leq Ch^3 |u|_{1,\infty,G} \\ &= Ch^3 \max_{x \in G} |\nabla \cdot \tilde{u}(x)| = C \theta_G \end{aligned} \quad (3.6)$$

3.3 Numerical Experiments - An r-method. We shall now cite some representative examples in which the r-method described above is used. All examples here are steady-state problems and the following conventions are used:

1. The numerical solution is computed on a fixed mesh and is advanced in time until a steady state is reached.

2. After convergence to a steady state, initial error indicators  $\theta_e$  are computed according to

$$\theta_e = A_e \int_{\Omega_e} \nabla \rho^h \cdot \nabla \rho^h d\Omega$$

in analogy with (3.5).

3. Then, a modified error indicator  $\tilde{\theta}_e$  is employed which is designed to be always greater than unity even when  $\theta_e \approx 0$ . In particular, we use

$$\tilde{\theta}_e = 1 + \frac{\alpha \theta_e}{\beta + \gamma \theta_e}$$

In our examples,  $\alpha = 81$ ,  $\beta = 1$ , and  $\gamma = 8$ .

4. Nodes are redistributed a total of K times using the procedure described earlier. In the example, we take only two iterations ( $K = 2$ ).

A Shock Reflection Problem. We begin with a problem for which an exact solution is known and which has been used as a benchmark problem by others.

The problem involves the steady flow of a perfect gas in a rectangular duct in which density, velocity, and energy are prescribed in each of four triangular wedges in such a way that the appropriate jump conditions (the Rankine-Hugoniot conditions) are exactly satisfied. Thus, a problem of shock reflection for which an exact solution is known is obtained. Dimensions and data are given in Fig. 2. In this and all the other problems, the solution is considered to have converged to steady state when the magnitude of the  $L^2$ -norm of the density is reduced by three orders of magnitude.

The time step is monitored by the formula

$$\Delta t = \min_e \left\{ \frac{0.50\sqrt{A_e}}{|\underline{u}| + C} \right\}$$

Here,  $C^2 = \frac{\gamma P}{\rho}$  and  $|\underline{u}|^2 = u_1^2 + u_2^2$ ,  $\gamma = 1.40$ . The constants multiplying the artificial viscous terms were selected locally as:

$$\tau_x = A_e \left| \overline{\frac{\partial u^n}{\partial x}} \right|_e, \quad \tau_y = A_e \left| \overline{\frac{\partial v^n}{\partial y}} \right|_e$$

where the bar denotes average element values. A Lapidus constant of 1.0 is used.

The results of a uniform coarse grid approximation are shown in Fig. 3. The computed density contours are also shown.

The same problem was also analyzed using the node redistribution algorithm with 20 node redistribution iteration. Results are shown in Fig. 4. There, the original coarse initial mesh of Fig. 3 is progressively

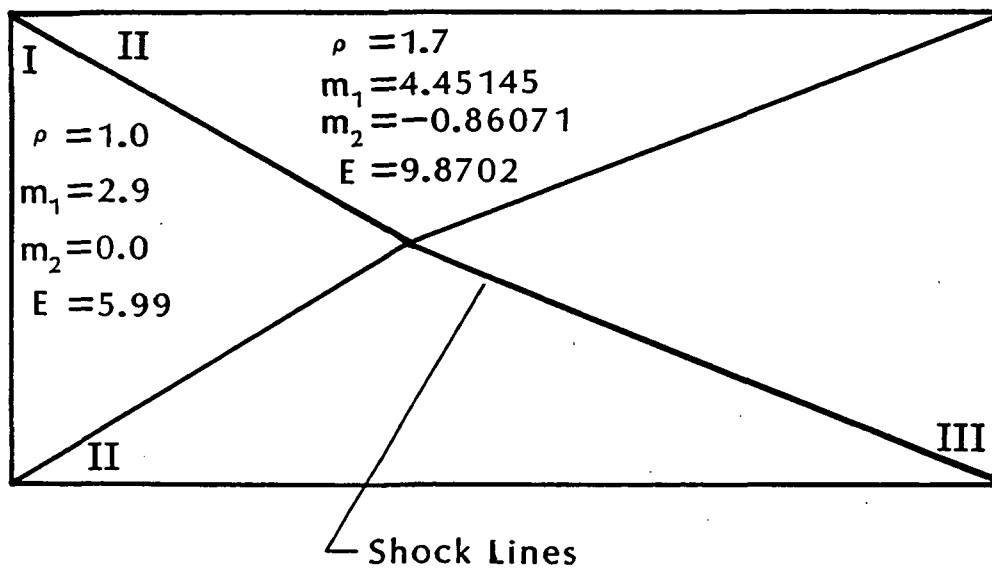


Figure 2. A shock reflection problem. Inflow values of the conservation variables are prescribed as indicated in regions I and II, and outflow values are computed in III to satisfy the conservation laws.



distorted to conform to the reflected shock locations. Corresponding density contours are also given in the figure.

NACA 0012 Airfoil in Supersonic Wind Tunnel. In this example, the supersonic flow through a narrow wind tunnel containing a NACA 0012 airfoil is studied. The inflow Mach number was set at  $M_\infty = 2$ , with  $\gamma = 1.40$  and symmetry is exploited to reduce the computational effort.

The initial coarse mesh and density computed contours are given in Fig. 5. Note that the critical features of the solution -- the reflected shock and contact discontinuity -- are lost with this coarse mesh. Results of a node-redistribution scheme for the coarse mesh are shown in Fig. 6. In these results, ten iterations of the node redistribution algorithm were used.

Supersonic Flow in a Wind Tunnel with a Step. The steady-state solution of the problem of a wind tunnel with a step introduced into the flow is next considered. The inflow Mach number was selected  $M_\infty = 3.0$  and  $\gamma = 1.40$ . The initial coarse mesh is shown in Figure 14 with the corresponding density profiles. The mesh refinement algorithm was also used, with the mesh and density profiles obtained after 10 iterations shown in Fig. 8. We see that some oscillations are present downstream, and they are believed to be due to the non-monotonicity of the solution algorithm. The results presented for the refinement-unrefinement procedure have been constrained by a maximum number of 2000 nodes or 2000 elements that can be allowed. In the refined mesh shown, this constraint has been achieved.

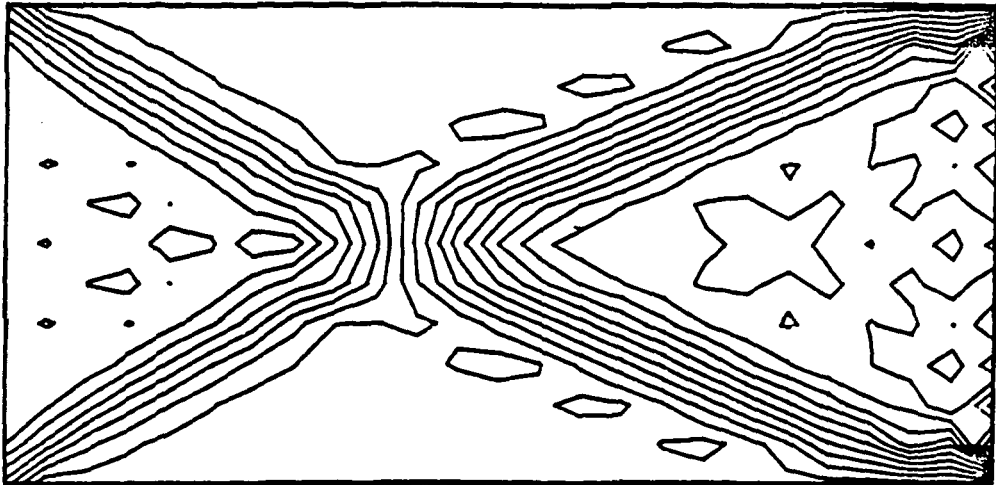
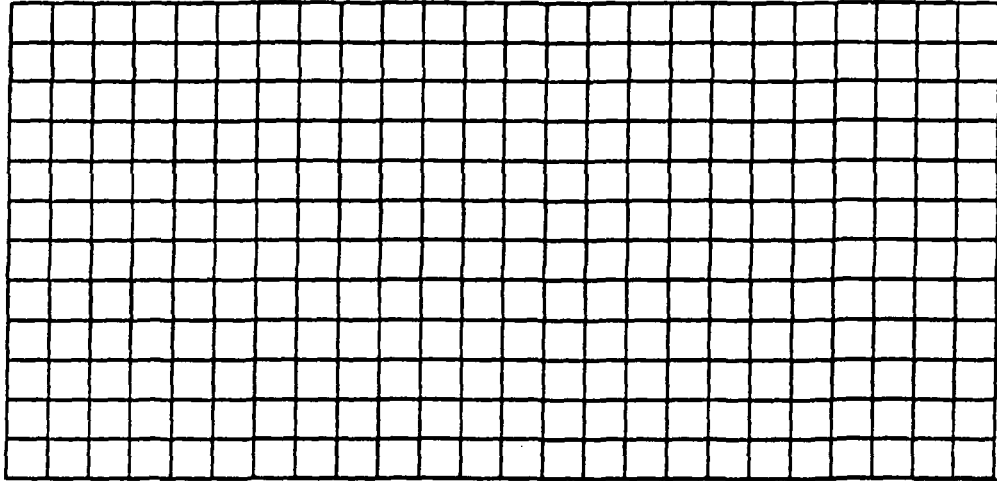


Figure 3. Reflecting shock problem.  
Initial mesh and density contours.

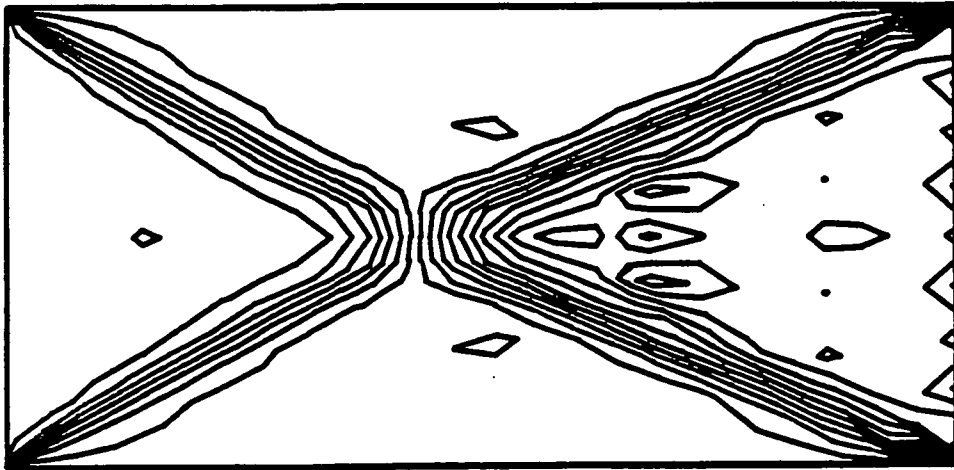
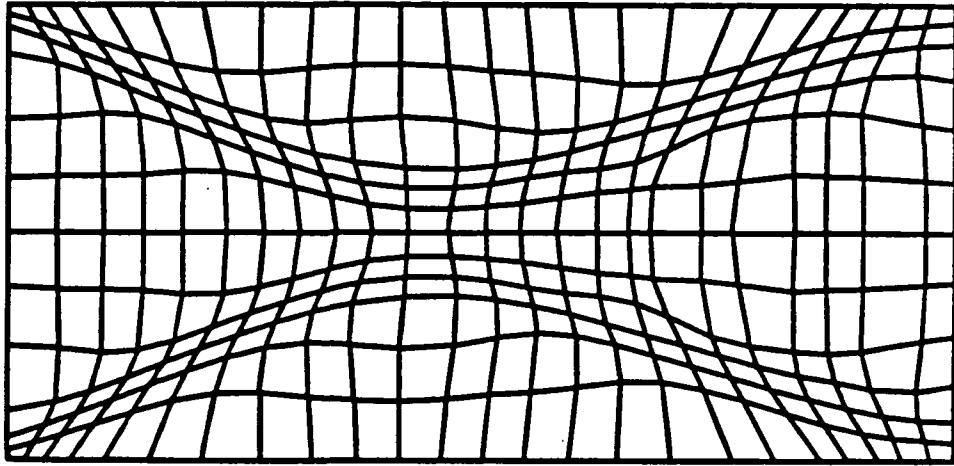


Figure 4. Reflecting shock problem. Mesh and density contours obtained after  $2 \times 10$  applications of the mesh redistribution algorithm.

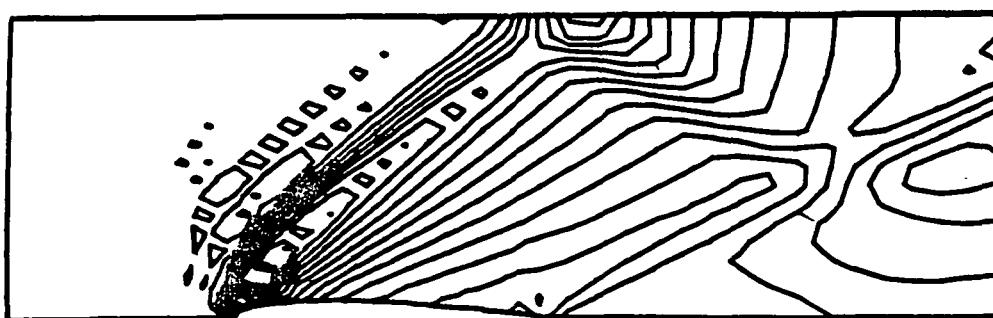
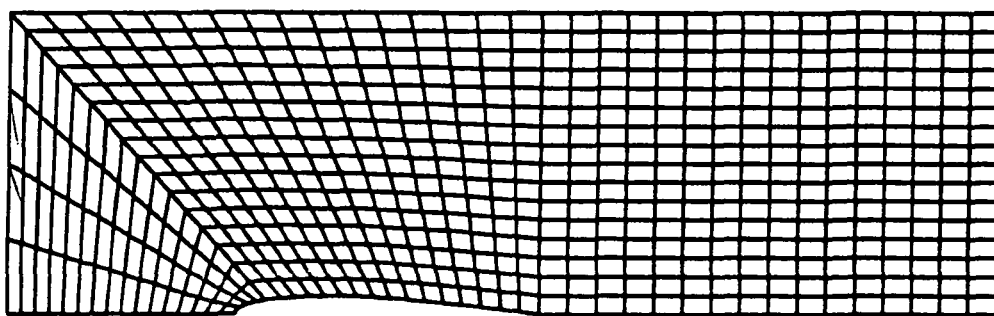


Figure 5. NACA 0012 airfoil in supersonic wind tunnel.  
Initial mesh and density contours.

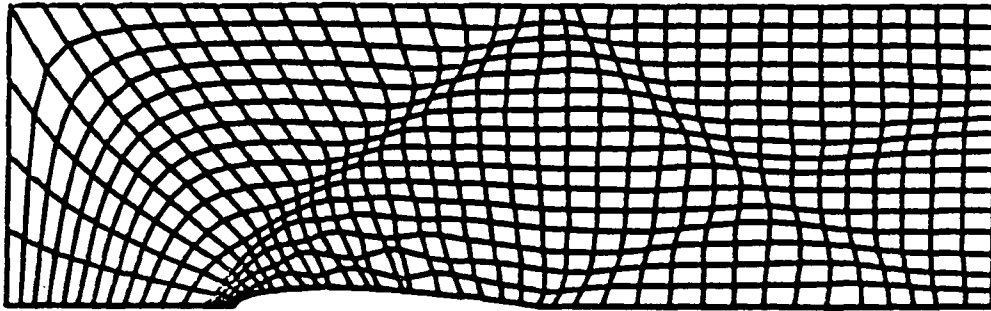


Figure 6. NACA 0012 airfoil in supersonic wind tunnel.  
Mesh and density contours obtained after  $2 \times 10$   
applications of the mesh redistribution algorithm.

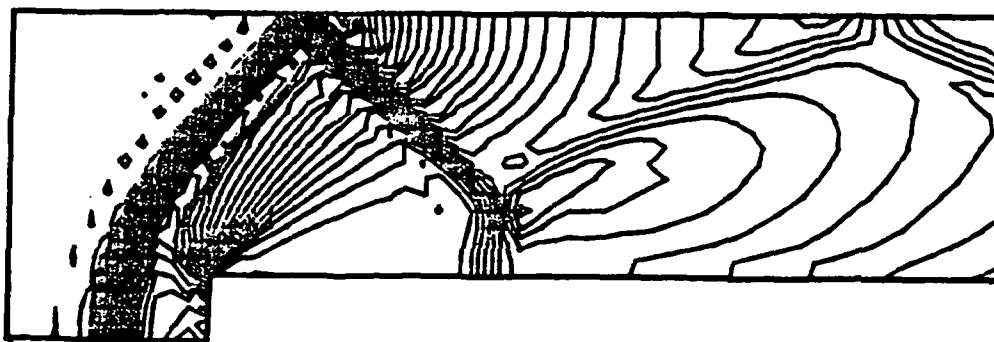
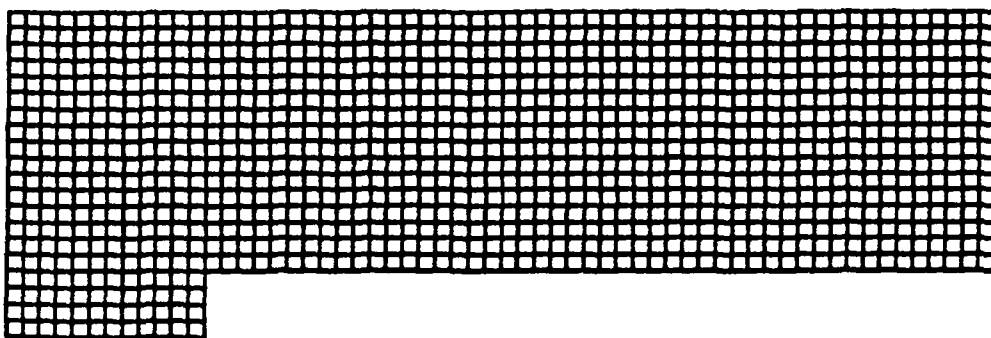


Figure 7. Supersonic flow in a wind tunnel with a step. Initial mesh and density contours.

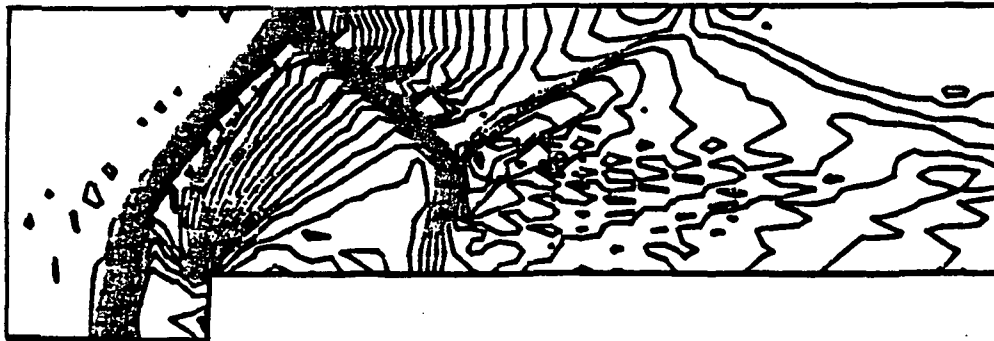
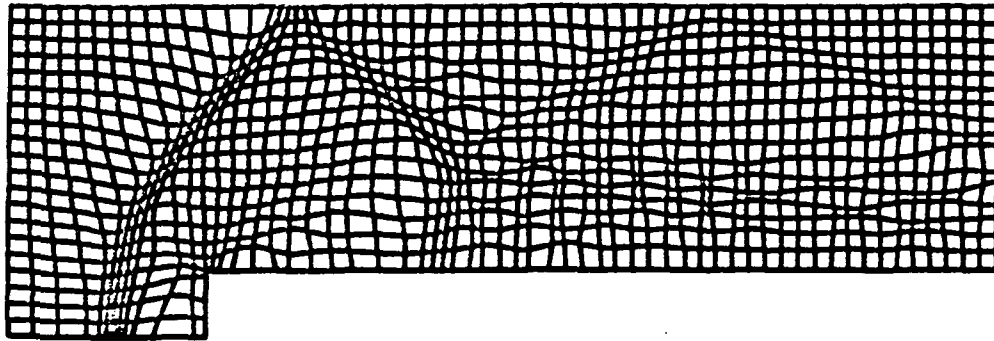


Figure 8. Supersonic flow in a wind tunnel with a step.  
Mesh and density contours obtained after  $2 \times 10^4$   
applications of the mesh redistribution algorithm.

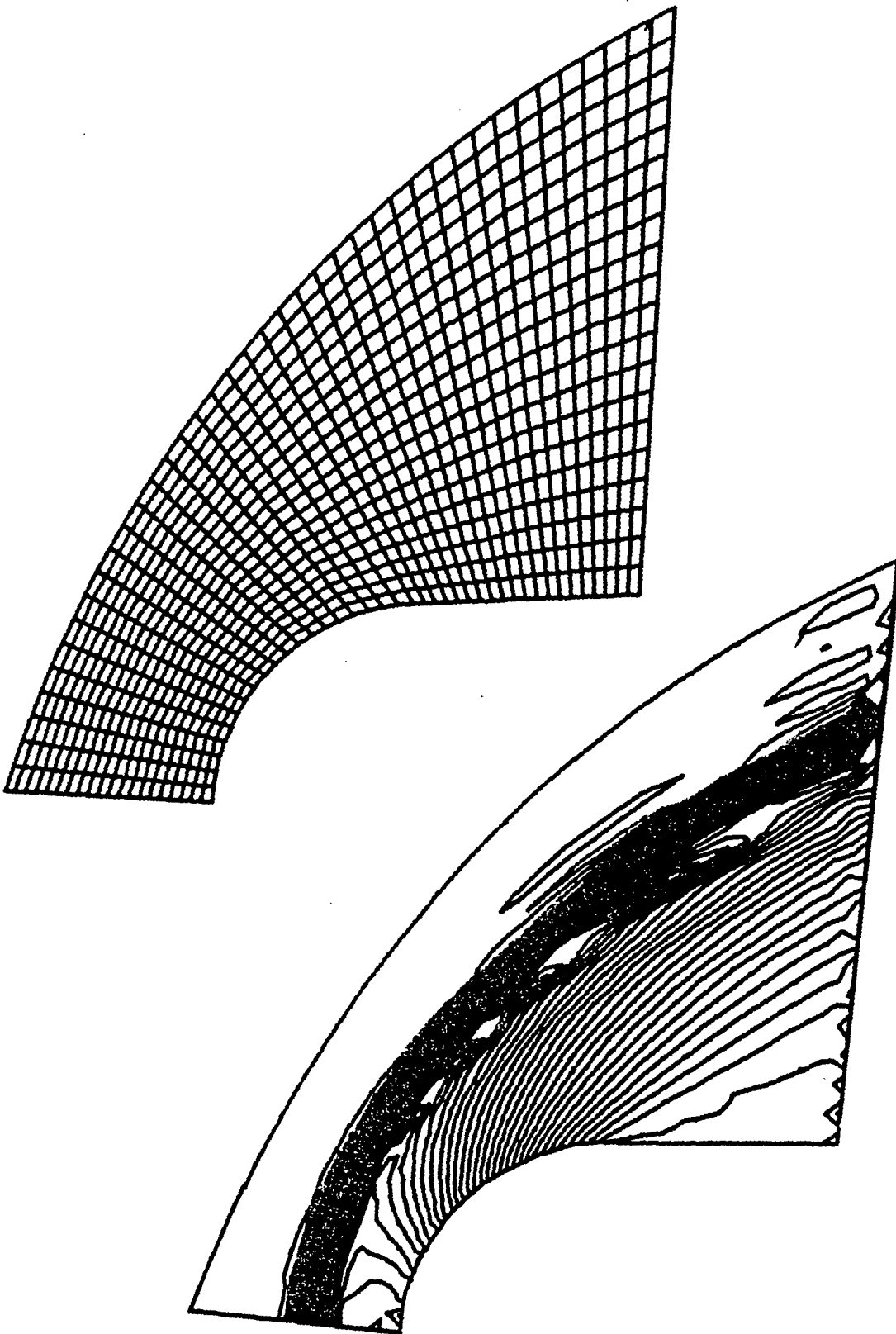


Figure 9. Blunt leading edge in hypersonic flow field.  
Initial mesh and density contours.



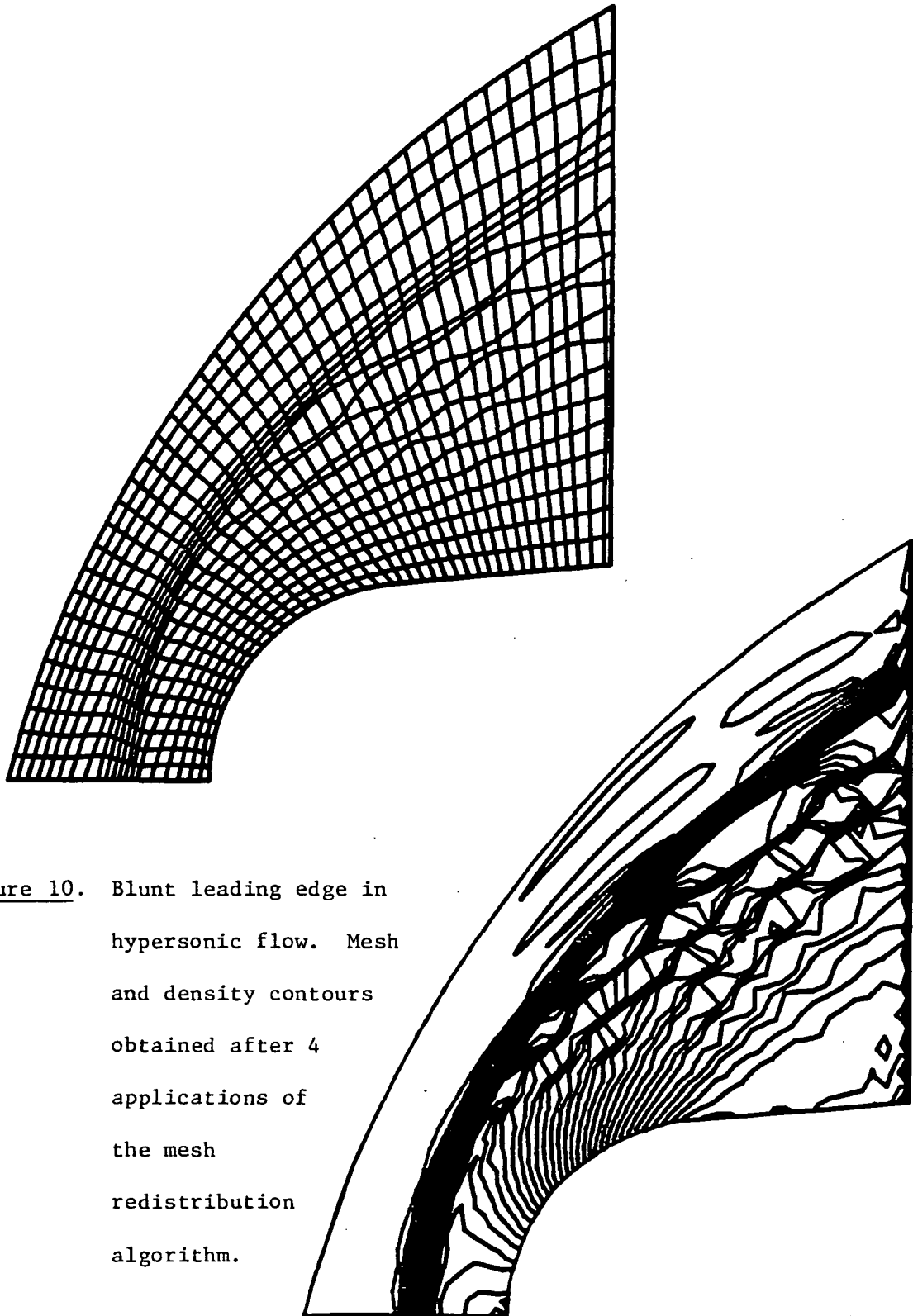


Figure 10. Blunt leading edge in hypersonic flow. Mesh and density contours obtained after 4 applications of the mesh redistribution algorithm.

### Blunt Leading Edge of 8' HTT Panel Holder in Hypersonic Flow.

The problem of the blunt leading edge of the 8' HTT panel holder in a supersonic flow field with freestream Mach number  $M_\infty = 6.57$ ,  $\gamma = 1.38$  and  $0^\circ$  angle of attack was solved to obtain the steady-state solution. This problem has also been studied by Bey et al.

A coarse mesh solution is indicated in Fig. 9. A distorted mesh and corresponding density map are indicated in Fig. 10. In this particular problem, the r-method did not give particularly good results, as a poor approximation of the solution between the shock and blunt body results from spurious oscillations in the basic time-marching algorithm. In the case of mesh adaptation using redistribution, the solution actually diverges after four passes through the adaptive scheme due to the badly graded (hourglassed) mesh produced from the oscillations of the adaptive scheme downstream of the shock.

3.4. A p-Method. Returning now to the full, viscous, Navier-Stokes problem characterized by (2.1), we outline a p-method for adaptive improvement of finite element solutions. The procedure is straightforward:

1. On a fixed mesh, compute a trial solution at each time step using a linear or bilinear approximation of the velocity field  $U_h^\epsilon$ .
2. Use  $U_h^\epsilon$  to compute a residual for data in a local problem which yields the local error indicator  $\phi_K$  over each element  $K$ .
3. Use local quadratic approximations to compute approximate error indicators  $\phi_K$ .

4. Check for pre-assigned error tolerances. If the error is too large, recompute  $U_h^\varepsilon$  locally using quadratic elements.

We employ hierarchal families of elements and could go up to quadric polynomials. In results given below, only quadratics are employed, and mesh refinement is used if increasing  $p$  fails to bring error with acceptable limits.

To test the residual estimation technique and our  $p$ -method, we examine the performance of the method using a problem with a known analytical solution. Since few analytical solutions to the transient Navier-Stokes equations are known, we attempt to construct solutions to special problems by choosing an analytic solution and then computing the corresponding boundary conditions and body force.

The theoretical analysis suggests the following local error indicators:

$$\varepsilon_{K,n}^0 = \left( \int_{t_{n-1}}^{t_n} \frac{(\rho |\phi^K|_{K,t}^2 + \rho |\frac{\partial \phi^K}{\partial t}|_{-1,K,t}^2 + \nu \|\phi^K\|_t^2) dt}{2} + \frac{\rho |\phi^K|_{K,t_n}^2 + \rho |\phi^K|_{K,t_{n-1}}^2}{2} \right)^{\frac{1}{2}}$$

$$\varepsilon_{K,n}^1 = |\phi^K|_{K,t_n}$$

$$\varepsilon_{K,n}^2 = \left( \int_{t_{n-1}}^{t_n} \|\phi^K\|_{K,t}^2 dt \right)^{\frac{1}{2}}$$

$$\varepsilon_{K,n}^3 = \left( \int_{t_{n-1}}^{t_n} |\frac{\partial \phi^K}{\partial t}|_{-1,K,t}^2 dt \right)^{\frac{1}{2}}$$

$$\varepsilon_{K,n}^4 = \left( \int_{t_{n-1}}^{t_n} |\phi^K|_{K,t}^2 dt \right)^{\frac{1}{2}}$$

Here,

$$|\phi^K|_{K,t}^2 = (\phi^K, \phi^K)_t; \|\phi^K\|_{K,t}^2 = ((\phi^K, \phi^K))_t$$

For each error indicator  $\varepsilon_{K,n}^j$ ,  $j = 1, \dots, 4$  we define the effectivity ratio

$$\theta_{K,n}^j = \frac{\varepsilon_{K,n}^j}{\|e_h\|_{K,n}^j}$$

where  $\|e_h\|_{K,n}^j$  is the norm estimated by  $\varepsilon_{K,n}^j$  as described above. We say that  $\varepsilon_{K,n}^j$  is an effective estimator if the corresponding effectivity ratio takes values close to unity.

In the numerical example to follow space-time elements of first order (bilinear in space, linear in time) are used to obtain an approximate solution and second-order space-time elements (biquadratic in space, quadratic in time) are employed to solve the local parabolic problems in the first time step. Then a normalized value  $\varepsilon_{K,n}^0$  of the local error indicator  $\phi^K$  is computed for every element  $K$ . A new order of approximation for element  $K$  is defined as follows:

If  $0 < \varepsilon_{K,n}^0 < \delta$  first order approximation

If  $\delta < \varepsilon_{K,n}^0 < 1$  second order approximation

Thus, the order of approximation is increased in the elements with error indicator bigger or equal to  $\delta$  times the value of the largest error indicator and an enriched mesh is obtained. This enriched mesh is used to advance the solution for  $M$  time steps (including the first) and after that the whole procedure is repeated. The success of this strategy in any particular problem depends on the choice of the

discretization parameters  $h$ ,  $\Delta t$  and the constants  $\delta$ ,  $M$ .

We now consider a problem with a one-dimensional "wave-like" solution in the fixed spatial domain  $\Omega = [0,20] \times [0,20]$ , namely

$$u = 0, v = 10e^{-\{0.8(x-4)-2t\}^2}, p = 0$$

The problem was solved with two uniform ( $5 \times 5$  and  $10 \times 10$ ) meshes using the following parameters:

Time step:  $\Delta t = 0.025, 0.100$

Penalty parameter:  $\varepsilon = 10^{-3}$

Fluid constants:  $\rho = 1, \mu = 1$

Kinematic boundary conditions were applied on the side with  $y = 0$  while traction boundary conditions were applied on the remaining three sides of the boundary. This explains why the numerical solution for the  $v$ -component shown in Fig. 11, 12 is not uniform in the  $y$ -direction.

For each error indicator we may compute a global effectivity ratio defined by:

$$\theta_n^j = \left( \frac{\sum_K (\varepsilon_{j,n}^K)^2}{\sum_K (\|e_h\|_{K,n}^j)^2} \right)^{1/2}$$

Table 1 gives the evolution of the global effectivity ratios for the proposed error estimators through the first nine time steps. It is observed that the values of these ratios diverge from the optimal value of one as the time marching progresses. This phenomenon is due to accumulation of the truncation error which destroys the effectivity of the error estimates and makes the adaptive procedure inefficient as

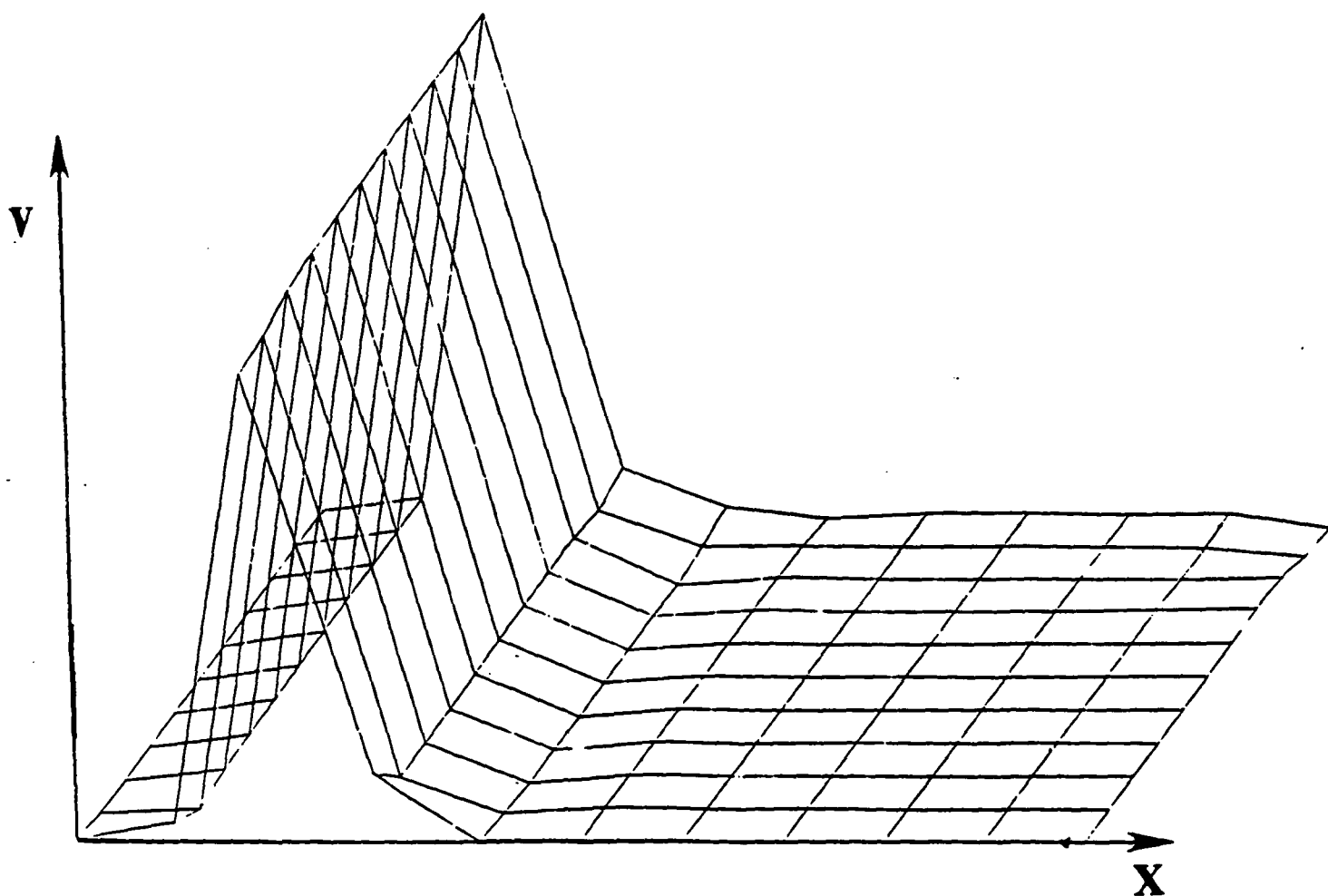


Figure 11. Problem with exponential solution. Computed solution for  
time  $t = 0.1$ . Parameters:  $h = 2$ ,  $\Delta t = 0.1$ ,  $\delta = 0.25$ ,  
 $M = 4$ .

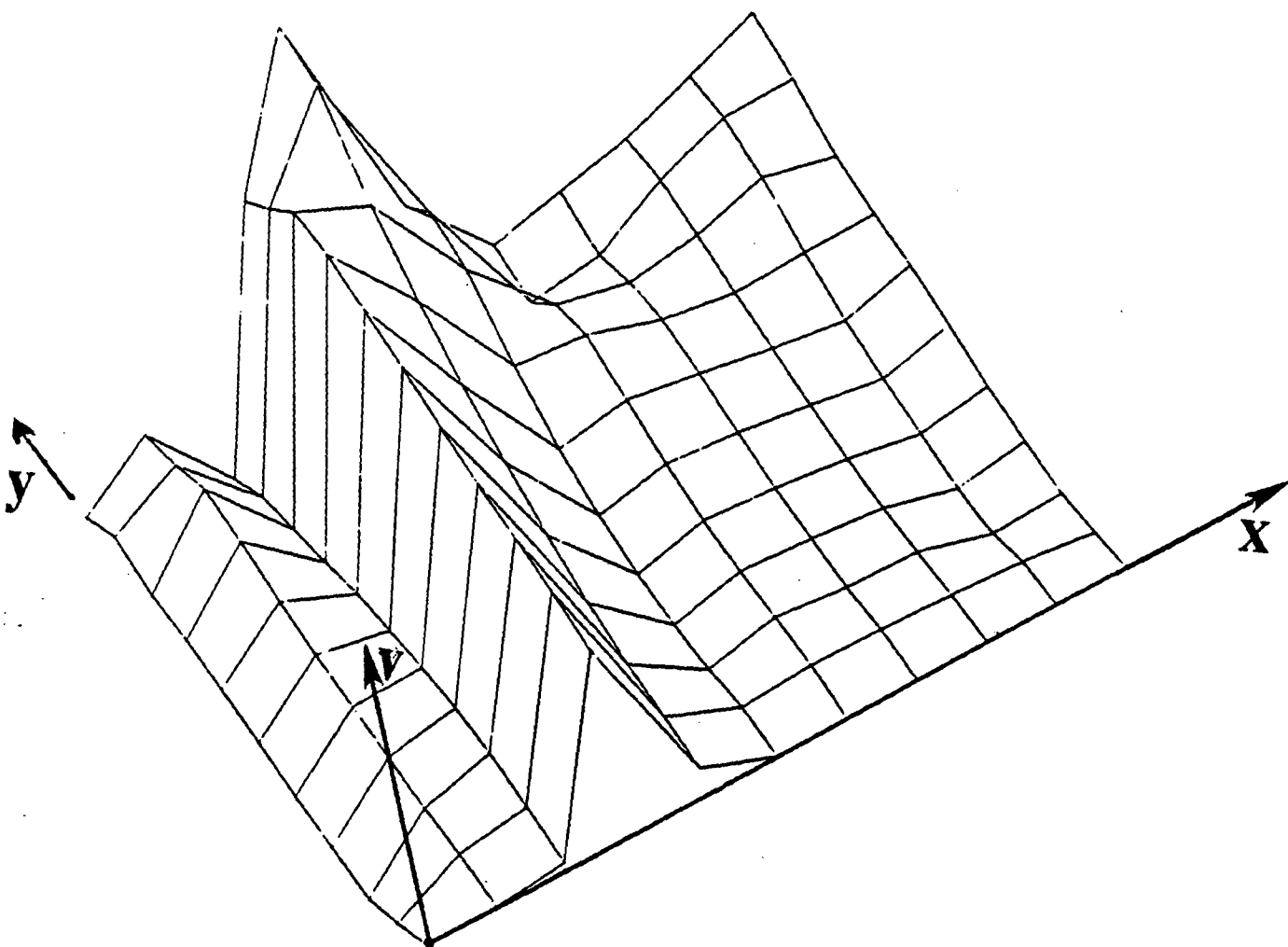


Figure 12. Problem with exponential solution. Computed solution for time  $t = 0.9$ . Parameters:  $h = 2$ ,  $\Delta t = 0.1$ ,  $\delta = 0.25$ ,  $M = 4$ .

can be seen. This situation can be corrected by reducing the values of the parameters of the adaptive procedure, namely  $h$ ,  $\Delta t$ ,  $M$ ,  $\delta$ .

Table 3.1

Values of the global effectivity ratios after the first time step;  $\Delta t = 0.025$

Mesh	$\theta_1^1$	$\theta_1^2$	$\theta_1^3$	$\theta_1^4$
5x5	1.0439	1.6995	1.3037	1.0339
10x10	1.0054	0.3225	1.1627	1.0011



#### 4. CONCLUSIONS

1. The use of rigorous residual error estimates for time-dependent Navier-Stokes problems in two dimensions is justified by the methods and results developed during the course of the work. In particular, sharp error bounds can be derived which were found to yield excellent error estimates for a test problem.

2. The use of p-methods and residual error estimates can be computationally expensive. New data structures must be developed before these types of methods can find wide application in practical flow problems.

3. Adaptive p-methods may ultimately offer significant advantages over other adaptive schemes if used in parallel computation with efficient use of multiple array processes. At present, these schemes do not perform well in comparison with some other adaptive strategies from the viewpoint of programming ease and computational efficiency.

4. Node redistribution methods are simple to use and can be effective in certain steady problems. They do not appear to be attractive in general flow problems, particularly in cases in which boundary conditions vary in time.

5. The node-redistribution-relaxation scheme described in this report can exhibit numerical instabilities in certain flow problems. The method is incapable of reducing local errors below very high tolerance levels without acquiring some destabilizing properties. It is doubtful that the method will find broad applications unless it is combined with an h-type or p-type adaptive strategy.

6. The h-methods, not dealt with here, do offer some advantages in terms of speed of implementation and general data structures over the r-method and the p-method developed here. However, these schemes can also exhibit instabilities. It is highly likely that the best adaptive schemes will prove to be those which combine h- and r-strategies.

7. Interpolation methods for error estimates are rather easy to implement and can be easily added to existing CFD software. They can provide only a crude indication of the actual local errors, but they can be used to produce an adequate indication of relative error between successive meshes.

8. Additional studies are needed to explore algorithms for accurate and efficient time-dependent problems. While we have developed some schemes in earlier work (e.g. [1]), a general approach to this important problem which fulfills requirements of accuracy and efficiency is not yet available.

#### REFERENCES

1. Oden, J.T., Robertson, S.J., Strouboulis, T., Devloo, Ph., Spradley, L.W. and McConnaughey, H.V., "Adaptive and Moving Mesh Finite Element Methods for Flow Interaction Problems", Proceedings, Sixth International Conference on Finite Element Methods in Fluids, Antibes, France, 1986 (to appear)
2. Oden, J.T., Strouboulis, T. and Devloo, Ph., "Adaptive Finite Element Methods for the Analysis of Inviscid Compressible Flow: I. Fast Refinement / Unrefinement and Moving Mesh Methods for Unstructured Meshes", TICOM Report, 863, The University of Texas at Austin, 1986
3. Demkowicz, L., Oden, J.T. and Strouboulis, T., "Adaptive Finite Element Methods for Flow Problems with Moving Boundaries. Part I: Variational Principles and A-Posteriori Estimates", Comput. Meths. Appl. Mech. Engrg., 46, 1984

4. Demkowicz, L., Devloo, Ph. and Oden, J.T., "On an h-Type Mesh Refinement Strategy Based on Minimization of Interpolation Errors", Comput. Meths. Appl. Mech. Engrg., 1985.
5. Oden, J.T., Demkowicz, L., Strouboulis, T. and Devloo, Ph., "Adaptive Methods for Problems in Solid and Fluid Mechanics", in L. Babuska, O.C. Zienkiewicz, J.P. de S.R. Gago and A. de Oliveira, Adaptive Methods and Error Refinement in Finite Element Computations, John Wiley and Sons, Ltd., London, 1986.
6. Donea, J., "A Taylor Galerkin Method for Convective Transport Problems", Internat. J. Numer. Meths. Engrg., 20, 1984.
7. Baker, A.J. and Kim, J.W., "Analyses on a Taylor Weak-Statement Algorithm for Hyperbolic Conservation Laws", Technical Report, CFDL-/86-1, Comp. Fluid Dyn. Lab., University of Tennessee, 1986
8. Löhner, R., Morgan, K. and Zienkiewicz, O.C., "Adaptive Grid Refinement for the Euler and Compressible Navier-Stokes Equations", in I. Babuska, O.C. Zienkiewicz, J.P. de S.R. Gago and A. de Oliveira, (Eds.), Adaptive Methods and Error Refinement in Finite Element Computations, John Wiley and Sons, Ltd., London, 1986.
9. Löhner, R., Morgan, K. and Zienkiewicz, O.C., "An Adaptive Finite Element Procedure for Compressible Flow in Deforming Regions", Comput. Meths. Appl. Mech. Engrg., 51, 1985.
10. Oden, J.T. and Carey, G.F., "Finite Elements: Mathematical Aspects", Vol. IV, Prentice Hall, Englewood Cliffs, 1983.

## APPENDIX

### **A-Posteriori Error Estimation for a Class of One-Dimensional Elliptic Problems.**

Consider the model problem,

$$\left. \begin{aligned} -\frac{d}{dx} \left( a \frac{du}{dx} \right) + bu &= f \quad \text{in } (0,1) \\ u(0) &= u(1) = 0 \end{aligned} \right\} \quad (1)$$

where it is assumed that

$$0 \leq a_{\min} \leq a(x) \leq a_{\max} < +\infty \quad \forall x \in [0,1]$$

$$0 \leq b(x) \leq b_1 \quad \forall x \in [0,1].$$

Assuming  $a, a', b, f \in C([0,1])$  we have  $u \in C^2([0,1])$ .

Let us define the bilinear form,

$$a(u, v) = \int_0^1 \left( a \frac{du}{dx} \frac{dv}{dx} + buv \right) dx$$

Then  $u$  is the solution of the variational equation,

$$a(u, v) = \int_0^1 f v dx \quad \forall v \in H_0^1([0,1])$$

Moreover, we define the energy norm  $\|\cdot\|_E$  by,

$$\|v\|_E^2 = a(v, v) \quad \forall v \in H^1([0,1])$$

We discretize  $[0,1]$  using  $N$  linear element  $\Omega_j = [x_{j-1}, x_j]$ ,  $j=1, \dots, N$ , where  $0=x_0 < x_1 < \dots < x_{j-1} < x_j < \dots < x_N=1$ . Let  $V^h \subseteq H_0^1([0,1])$  denote the space which is spanned by the basis functions of the discretization. We approximate the solution  $u$  of (1) with a  $u_h \in V^h$  which is obtained as the solution of the discrete problem:

Find  $u_h \in V^h$  such that,

$$a(u_h, v_h) = \int_0^1 f v_h dx \quad \forall v_h \in V^h$$

We want to estimate the energy norm of the approximation error,

$e_h = u - u_h$ . In view of the orthogonality condition,

$$a(e_h, v_h) = 0 \quad \forall v_h \in V^h$$

the energy norm of the approximation error satisfies,

$$\|e_h\|_E^2 = a(e_h, e_h - v_h)$$

Choose  $\hat{v}_h \in V^h$  such that  $\hat{u}_h(x_j) = e_h(x_j)$ ,  $j=0,1,\dots,N$  and let  $w = e_h - \hat{u}_h$  to obtain:

$$\|e_h\|_E^2 = \sum_{j=0}^{N-1} \int_{x_j}^{x_{j+1}} \left\{ a \frac{d}{dx} (u - u_h) \frac{dw}{dx} + b(u - u_h)w \right\} dx \quad (2)$$

Integrating by parts and noting that  $u_h'' = 0$  in  $(x_j, x_{j+1})$ ,  $j=0,1,\dots,N-1$ , we get,

$$\|e_h\|_E^2 = \sum_{j=0}^{N-1} \int_{x_j}^{x_{j+1}} (f + a' u_h' - b u_h) w dx \quad (3)$$

We also have (see Babuska and Rheinboldt [1]) that:

$$\|e_h - \hat{v}_h\|_E \leq (1 + O(h)) \|e_h\|_E \quad (4)$$

Starting from (2) and using Schwarz's and Korn's inequality and (3) we get the following estimate:

$$\|e_h\|_E \leq (1+O(h)) K(h) \left( \sum_{j=0}^{N-1} \int_{x_j}^{x_{j+1}} (f+a'u'_h - bu_h)^2 dx \right)^{1/2} \quad (5)$$

Here,  $h = \max_{0 \leq i \leq N-1} (x_{i+1} - x_i)$ , and  $K(h)$  denotes Korn's constant.

The estimate given in (4) has the disadvantage that it involves Korn's constant which has to be computed for a given discretization and even then the estimate is far from being optimal. Babuska and Rheinboldt [2], developed a less obvious approach ( than the one leading to (4) ) which gives sharp error estimates. This approach is summarized below.

Define a family of local auxiliary problems as follows:

For every element  $\Omega_{j+1}$ , find  $\phi_{j+1} \in H_0^1([x_j, x_{j+1}])$  such that,

$$a(\phi_{j+1}, v) = \int_{x_j}^{x_{j+1}} (f+a'u'_h - bu_h) v dx$$

$$\forall v \in H_0^1([x_j, x_{j+1}]), j=0, \dots, N-1$$

Combining (2) with (5) using Schwarz's inequality and inequality (3) we obtain the bound:

$$\|e_h\|_E \leq \left( \sum_{j=0}^{N-1} \|\phi_{j+1}\|_{E, \Omega_{j+1}}^2 \right)^{1/2}$$

One can estimate  $\|\phi_{j+1}\|_{E, \Omega_{j+1}}$  using the Lax-Milgram theorem to obtain:

$$\|\phi_{j+1}\|_{E, \Omega_{j+1}} \leq C_{j+1} \|f+a'u'_h - bu_h\|_{0, \Omega_{j+1}}$$

Moreover by using spectral analysis one can show (see [3])

$$C_{j+1} \leq \frac{(x_{j+1}-x_j)^2}{\pi^2 \min_{x \in (x_j, x_{j+1})} a(x)} \quad (6)$$

and finally we get the estimate:

$$\|e_h\|_E \leq \left[ \sum_{j=0}^{N-1} \frac{(x_{j+1}-x_j)^2}{\pi^2 \min_{x \in (x_j, x_{j+1})} a(x)} \|f+a'u'_h-bu_h\|_{0,\Omega_{j+1}}^2 \right]^{1/2} \quad (7)$$

We note that the error bound given in (6) can be computed without solving the local problems defined in (5).

### Locally Computed A-Posteriori Error Estimates for Elliptic Equations

For the sake of simplicity, we first restrict ourselves to the following model elliptic problem.

Find  $u$  such that

$$\Delta u = f \text{ in } \Omega$$

$$u = u_0 \text{ on } \Gamma_u$$

$$\frac{\partial u}{\partial n} = g \text{ on } \Gamma_T$$

Here  $\Omega$  is a bounded domain in  $\mathbb{R}^2$ ,  $\Gamma_u$ , and  $\Gamma_T$  form two disjoint parts of the boundary  $\partial\Omega$  and  $f$ ,  $u_0$ ,  $g$  are given functions.

If  $u_0$  denotes a function from  $H^1(\Omega)$  whose extension to  $\Gamma_u$  coincides

with  $u_0$  ( when we use the same symbol for  $u_0$  and its extension) we have the usual variational formulation to (7).

Find  $u \in u_0 + V$  such that

$$\int_{\Omega} \nabla u \cdot \nabla v \, d\Omega = \int_{\Omega} f \cdot v \, d\Omega + \int_{\Gamma_T} g v \, ds \quad \forall v \in V$$

where

$$V = \{u \in H^1(\Omega) | u = 0 \text{ on } \Gamma_u\}$$

and  $d\Omega$ ,  $ds$  denote measures of volume and surface area respectively.

In the following, we discuss a method to compute a-posteriori error estimates for finite element solutions of (7).

Suppose we are given two approximation spaces, say  $V_h^1, V_h^p \subset V$  such that approximation (interpolation particularly) of an arbitrary element  $v \in V$  by elements  $v_h^p \in V_h^p$  results in "much smaller" error than the approximation by  $v_h^1 \in V_h^1$ . Specifically we can think about  $V_h^p$  as the space spanned by the hierarchical elements with order  $p$  large enough.  $V_h^1$  does not mean necessarily the space corresponding to the first order approximation.

The approximate problem for the "lower order" approximation can be stated as follows:

Find  $u_h^1 \in u_0 + V_h^1$  such that



$$\int_{\Omega} \nabla u_h^1 \cdot \nabla v_h^1 d\Omega = \int_{\Omega} f v_h^1 d\Omega + \int_{\Gamma_T} g v_h^1 ds \quad \forall v_h^1 \in V_h^1$$

For simplicity, we will assume that kinematic boundary conditions can be satisfied **exactly** by the first order approximation (i.e.,  $u_0 \in V_h^1$ ).

The residual  $r_h^1$  corresponding to the solution  $u_h^1$  is an element from the dual space  $V^*$  and should be estimated in the corresponding dual space norm:

$$\|r_h^1\|_{V^*} = \sup_{\substack{v \in V \\ \|v\|_V \leq 1}} \langle r_h^1, v \rangle \quad (8)$$

Certainly  $r_h$  is weakly continuous over  $V$  and the ball  $\|v\|_V \leq 1$  is weakly compact, and, therefore, there must exist a certain  $v_0$ ,  $\|v_0\|_V \leq 1$  in fact it must be normalized in the sense that  $\|v_0\| = 1$ ) such that

$$\|r_h\|_{V^*} = \langle r_h^1, v_0 \rangle$$

Now, let  $\hat{v}_{0_h}^p$  denote the best approximation of  $v_0$  out of the space  $V_h^p$ . Suppose

$\|v_0 - \hat{v}_{0_h}^p\| \leq \varepsilon$ . Defining  $v_{0_h}^p = \hat{v}_{0_h}^p / \|\hat{v}_{0_h}^p\|$  we easily conclude that also

$$\|v_0 - v_{0_h}^p\| \leq \varepsilon + \frac{\varepsilon}{1-\varepsilon}$$

which is equivalent to saying that  $v_0$  can be approximated "close enough" by elements with unit norm.

Next, (8) can be replaced by

$$\|r_h^1\|_V \leq \|r_h^1\|_V \|v_0 - v_h^p\| + \sup_{\|v_h^p\| \leq 1} \langle r_h^1, v_h^p \rangle \quad (9).$$

the first term on the right-hand side being negligible. In other words we presume that the error in terms of the dual space norm can be estimated sufficiently well by taking the supremum over only the subspace  $V_h^p$ .

Now let us try to estimate this supremum. We have:

$$\begin{aligned} \langle r_h^1, v_h^p \rangle &= \int_{\Omega} \nabla u_h^1 \cdot \nabla v_h^p \, d\Omega - \int_{\Omega} f v_h^p \, d\Omega - \int_{\partial\Omega} g v_h^p \, ds = \\ &= \sum_K \left\{ \int_K (-\Delta u_h^1 - f) v_h^p \, d\Omega + \int_{\partial K \cap \partial\Omega} \frac{1}{2} \left( \frac{\partial u_h^1}{\partial n} - \frac{\partial u_h^{1*}}{\partial n} \right) v_h^p \, ds + \right. \\ &\quad \left. + \int_{\partial K \cap \Gamma_T} \left( \frac{\partial u_h^1}{\partial n} - g \right) v_h^p \, ds \right\} \quad (2.n+y) \end{aligned}$$

Let us note also that in (2.24)  $v_h^p$  can be replaced by the difference  $v_h^p - v_h^1$ , with arbitrary  $v_h^1 \in V_h^1$  since the residual  $r_h^1$  is orthogonal to  $V_h^1$ . In particular, we can choose for  $v_h^1$  a  $V_h^1$ -interpolant of  $v_h^p$ .

Finally, defining

$$V_{h_0}^p(K) = \{v_h^p \in V_h^p(K) \mid V_h^1\text{-interpolant of } v_h^p = 0\}$$

we may use the following local problem associated with an element  $K$ :

Find  $\phi_K \in V_{h_0}^p(K)$  such that:

$$\begin{aligned}
& \int_K \nabla \phi_K \nabla v_h^p \, d\Omega = \\
& \int_K (-\nabla u_h^1 - f) v_h^p \, d\Omega + \int_{\partial K \cap \partial \Omega} \frac{1}{2} \left( \frac{\partial u_h^1}{\partial n} - \frac{\partial u_h^{1*}}{\partial n} \right) v_h^p \, ds \\
& + \int_{\partial K \cap \Gamma_T} \left( \frac{\partial u_h^1}{\partial n} - g \right) v_h^p \, ds \quad \forall v_h^p \in V_h^p(K)
\end{aligned}$$

and equation (9) can be rewritten in the form:

$$\langle r_h^1, v_h^p \rangle = \sum_K \int_K \nabla \phi_K \nabla (v_h^p - v_h^1) \, d\Omega$$

The functions  $\phi_K$  are *local error indicator functions*.

Finally, we note that for each element  $K$  there exists a constant  $C_K$  such that

$$\|v_h^p - v_h^1\|_{1,K} \leq C_K \|v_h^p\|_{1,K} \quad \forall v_h^p \in V_h^p(K)$$

which results in

$$\langle r_h^1, v_h^p \rangle \leq C \left( \sum_K \int_K (\nabla \phi_K)^2 \, d\Omega \right)^{1/2} \|v_h^p\|_V \quad (10)$$

provided

$$C = \max_K C_K$$

The constant  $C_K$  is independent of the size of element  $K$ , but it does depend on its shape. In particular, for grids consisting of the same regular elements (not necessarily uniform  $C_K$  is independent of  $K$  and does not affect the local

behavior of the estimate (10) (comp. also [ 4 ]).

Our estimate:

$$\|r_h^1\|_V \leq C \left( \sum_K \int_K (\nabla \phi_K)^2 d\Omega \right)^{1/2}$$

clearly has only a global character; however, the contributions  $\int_K (\nabla \phi_K)^2 d\Omega$  (local) error indicators) may serve as a basis for some local refinement.

Finally, let us note that in the case of the model problem the residual estimate *can be directly reinterpreted* as the estimate of the error  $e_h^1 = u_h^1 - u$ , since

$$\begin{aligned} \|e_h^1\|_V^2 &= \int_{\Omega} \nabla e_h^1 \nabla e_h^1 d\Omega = \\ &= \int_{\Omega} \nabla u_h^1 \nabla e_h^1 d\Omega - \int_{\Omega} (-\Delta u) e_h^1 d\Omega - \int_{\Gamma_T} \frac{\partial u}{\partial n} e_h^1 ds = \\ \langle r_h^1, e_h^1 \rangle &\leq \|r_h^1\| \cdot \|e_h^1\| \end{aligned}$$

and therefore,

$$\|e_h^1\|_V \leq \|r_h^1\|.$$

Conversely taking into account that in the case of a Hilbert space  $H$  with inner product  $(\cdot, \cdot)_H$  and the corresponding norm  $\|\cdot\|_H$ ,

$$\|u\|_H = \sup_{v \in H} \frac{\langle u, v \rangle}{\|v\|}$$

one gets that

$$\|r_h^1\|_* = \|e_h^1\|_V \quad (11)$$

In fact, for any self-adjoint elliptic problem we may define the proper (energy) norm in such a way that the norm of residual is exactly equal to the norm of the error. For a class of not self-adjoint problems or for certain classes of nonlinear operators (strongly monotone) the residual norm can likewise be bounded below by the norm of the error. However, in general the relation between these two quantities is more complicated and we must be satisfied with the observation that, in general *when the solution of the boundary value problem depends continuously on the right-hand side (the data), it makes sense to minimize the residual since it results in simultaneous convergence of the approximate solution to the exact one* (see also [ 5 ]).

We now show that the concept of estimating the residual over a higher order approximation space  $V_h^p$  can be easily applied to Stokes problem. Stokes problem is of special interest to us since it is obtained from a linearization of the stationary Navier-Stokes equations.

Let us restrict ourselves to the case of pure kinematic boundary conditions (the Dirichlet problem). The Stokes consists in the determination of the velocity field  $u$  and pressure field  $p$  such that:

$$\begin{aligned}
-\mu \Delta \underline{u} + \text{grad } p &= \underline{f} \\
\text{div } \underline{u} &= 0 \quad \text{in } \Omega \\
\underline{u} &= \underline{u}_0 \quad \text{on } \partial\Omega
\end{aligned}$$

where  $\mu$  is the viscosity constant,  $\underline{f}$  stands for body forces and  $\underline{u}_0$  specifies velocity on the boundary. The usual consistency condition must be satisfied, i.e.,

$$\int_{\partial\Omega} \underline{u}_n \, ds = 0$$

where  $\underline{u}_n = \underline{u} \cdot \underline{n}$ , provided  $\underline{n}$  denotes the outward normal unit to  $\partial\Omega$ . The variational formulation of (2.32) is as follows:

Find  $\underline{u} \in \underline{u}_0 + V$ ,  $p \in L_0^2(\Omega)$  such that:

$$\begin{aligned}
\mu \int_{\Omega} \varepsilon_{ij}(\underline{u}) \varepsilon_{ij}(\underline{v}) \, d\Omega + \int_{\Omega} p \, \text{div } \underline{v} \, d\Omega &= \int_{\Omega} \underline{f} \underline{v} \, d\Omega \quad \forall \underline{v} \in V \\
\int_{\Omega} \text{div } \underline{u} \, q \, d\Omega &= 0 \quad \forall q \in L_0^2(\Omega)
\end{aligned}$$

Here  $\varepsilon_{ij}(\underline{u})$  denotes the symmetric part of the gradient of  $\underline{u}$ . In the above  $\underline{u}_0$  denotes an arbitrary function in  $H^1(\Omega)$ , such that  $\underline{u}_0|_{\partial\Omega} = \underline{u}_0$  (again, we use the same notation for  $\underline{u}_0$  and for its trace on the boundary, and that  $\text{div } \underline{u}_0 = 0$ , and  $V = H_0^1(\Omega)$  and, as usual,

$$L_0^2(\Omega) = \{q \in L^2(\Omega) \mid \int_{\Omega} q \, d\Omega = 0\}$$

Denoting, as previously, a  $p$ -th order approximation space by  $V_h^p$  and  $L_{0h}^{2p}$  respectively, we may formulate the  $p$ -th order approximate problem as follows:

Find  $u_h^p \in u_0^p + V_h^p$ ,  $p_h^p \in L_{oh}^2(\Omega)$ , such that

$$\begin{aligned} \mu \int_{\Omega} \epsilon_{ij}(u_h^p) \epsilon_{ij}(v_h^p) d\Omega + \int_{\Omega} p_h^p \operatorname{div} (v_h^p) d\Omega &= \int_{\Omega} f v_h^p d\Omega \quad \forall v_h^p \in V_h^p \quad (12) \\ \int_{\Omega} \operatorname{div} u_h^p q_h^p d\Omega &= 0 \quad \forall q \in L_{oh}^{1p} \end{aligned}$$

As in the preceding case, we attempt to estimate the proper residuals corresponding to the "1-st order approximation" i.e., replacing suprema over  $y \in V$  and  $q \in L_0^2(\Omega)$  by suprema over  $y_h^p \in V_h^p$  and  $q_h \in L_{oh}^{2p}$ , with some  $p > 1$ .

We have for the first equation:

$$\begin{aligned} < -\mu \Delta u_h^1 + \operatorname{grad} p_h^1 - f; y_h^p > = \\ \sum_K \{ \int_K \epsilon_{ij}(u_h^1) \epsilon_{ij}(y_h^p) d\Omega - \int_K p_h^1 \operatorname{div} y_h^p d\Omega - \int_K f y_h^p d\Omega \} = \\ \sum_K \{ \int_K (-\Delta u_h^1 + \operatorname{grad} p_h^1 - f) y_h^p d\Omega + \\ \int_{\partial K \cap \partial \Omega} \frac{t(u_h^1, p_u^1) - t^*(u_h^1, p_u^1)}{2} \cdot y_h^p ds \} \end{aligned} \quad (13)$$

where, as usual,  $t^*$  denotes a stress vector corresponding to an adjacent element.

For the second equation we get simply:

$$< \operatorname{div} u_h^1, q_h^p > = \sum_K \int_K \operatorname{div} u_h^1 q_h^p d\Omega$$

As usual, one can see that  $y_h^p$  and  $q_h^p$  in (12) and (13) can be replaced by

$y_h^p - y_h^1$  and  $q_h^p - q_h^1$  for arbitrary  $y_h^1$  and particularly choosing for  $y_h^1$  and  $q_h^1$  interpolants of  $y_h^p$  and  $q_h^p$  we can set the local problem in the following way:

Find  $\phi_K \in V_{h0}^p(K)$ ,  $\psi_K \in L_{h0}^p(K)$  such that:

$$\mu \int_K (-\Delta u_h^1 \text{ grad } p_h^1 - f) y_h^p \, d\Omega + \int_{\partial K} \frac{t-t^*}{2} y_h^p \, d\Omega \quad \forall y_h^p \in V_{h,0}^p(K)$$

$$\int_K \text{div}(\phi_K) q_h^p \, d\Omega = 0 \quad \forall q_h^p \in L_{h0}^p(K)$$

In the above  $V_{h0}^p(K) = \{u_h^p \in V_h^p(K) | V_h^1\text{-interpolant} = 0\}$

$$L_{h0}^p(K) = \{q_h^p \in L_h^p(K) | L_h^1\text{-interpolant of } q_h^p = 0\}$$

Finally (12) and (13) can be rewritten in the form:

$$\langle -\mu \Delta u_h^1 + \text{grad } p_h^1 - f, v_h^p \rangle =$$

$$\sum_K \left\{ \mu \int_K \epsilon_{ij}(\phi_K) \epsilon_{ij}(y_h^p - y_h^1) \, d\Omega - \int_K \psi_K \text{div}(y_h^p - y_h^1) \, d\Omega \right\}$$

and

$$\langle \text{div } u_h^1, q_h^p \rangle = \sum_K \int_K \text{div}(\phi_K)(q_h^p - q_h^1) \, d\Omega$$

where  $y_h^1$  and  $q_h^1$  are the appropriate interpolants of  $y_h^p$  and  $q_h^p$  respectively. Both identities lead to the residual error estimates. However, the second one is practically useless, since the  $\|\text{div } u_h^1\|_{L^2(\Omega)}$  can be estimated simply by a direct computation. Let us therefore focus our attention on the first residual. By Schwarz's inequality, we get



$$\begin{aligned}
& \left| \mu \int_K \varepsilon_{ij}(\phi_K) \varepsilon_{ij}(\mathbf{v}_h^p - \mathbf{v}_h^1) d\Omega - \int_K \psi_K \operatorname{div}(\mathbf{v}_h^p - \mathbf{v}_h^1) d\Omega \right| \leq \\
& \leq (\|\phi_K\|_{E,K}^2 + \|\psi_K\|_{0,K}^2)^{1/2} \|\mathbf{v}_h^p - \mathbf{v}_h^1\|_K \leq \\
& \leq C_K (\|\phi_K\|_{E,K}^2 + \|\psi_K\|_{0,K}^2)^{1/2} \|\mathbf{v}_h^p\|_K,
\end{aligned}$$

where  $\|\cdot\|_{E,K}$  is energy norm associated with the viscous, bilinear form,  $\|\mathbf{y}\|_K = (\|\mathbf{y}\|_{E,K}^2 + \|\operatorname{div} \mathbf{y}\|_{0,K}^2)^{1/2}$  is a well-defined norm in  $V_{ho}^p(K)$ , and finally  $C_K$  is a constant associated with the estimate of the type:

$$\|\mathbf{v}_h^p - \mathbf{v}_h^1\|_K \leq C_K \|\mathbf{v}_h^p\|_K \quad \forall \mathbf{v}_h^p \in V_h^p(K)$$

$C_K$  is independent of the size of the element  $K$  but depends upon its shape. For detailed discussion of these ideas, we refer to [4]. We note here that for meshes which are uniform or consist of elements of the same shape the constant  $C_K$  is independent of the element and does not affect the local behavior of the estimate.

Finally, we arrive at the estimate:

$$\|-\mu \Delta u_h^1 + \operatorname{grad} p_h^1 - f\|_{-1,\Omega} \leq C \left( \sum_K (\|\phi_K\|_{E,K}^2 + \|\psi_K\|_{0,K}^2) \right)^{1/2}$$

where  $C = \max_K C_K$ , and the norm in the dual space is measured with respect to the norm:

$$\|\mathbf{v}\| = \left( \sum_K (\|\mathbf{v}\|_{E,K}^2 + \|\operatorname{div} \mathbf{v}\|_{0,K}^2) \right)^{1/2}$$

#### REFERENCES FOR THIS APPENDIX

1. Babuska, I. and Rheinboldt, W.C., "Error Estimates for Adaptive Finite Element Computations", SIAM J. Numer. Anal., 15 (4), 1978.
2. Babuska, I. and Rheinboldt, W.C., "Analysis of Optimal Finite-Element Meshes in  $R^1$ ", Math. Comput., 36 (146), 1979.
3. Kelly, D.W., Gago, J.P. de S.R., Zienkiewicz, O.C. and Babuska, I., "A-Posteriori Error Analysis and Adaptive Processes in the Finite Element Method, Part II - Adaptive Mesh Refinement", Internat. J. Numer. Meths. Engrg., 19, 1983.
4. Demkowicz, L., Oden, J.T. and Strouboulis, T., "Adaptive Finite Element Methods for Flow Problems with Moving Boundaries. Part I: Variational Principles and A-Posteriori Estimates", Comput. Meths. Appl. Mech. Engrg., 46, 1984.
5. Oden, J.T., Demkowicz, L., Strouboulis, T. and Devloo, Ph., "Adaptive Methods for Problems in Solid and Fluid Mechanics", in I. Babuska, O.C. Zienkiewicz, J.P. de S.R. Gago and A. de Oliveira, Adaptive Methods and Error Refinement in Finite Element Computations, John Wiley and Sons, Ltd., London, 1986.